Chemical Engineering & Processing: Process Intensification 193 (2023) 109548

Contents lists available at ScienceDirect

Chemical Engineering and Processing - Process Intensification

journal homepage: www.elsevier.com/locate/cep

Process intensification in bio-jet fuel production: Design and control of a catalytic reactive distillation column for oligomerization

Gabriel Contreras-Zarazúa [a,b], Eduardo Sánchez-Ramirez [b], Esteban Abelardo Hernández-Vargas [c], Juan Gabriel Segovia-Hernández [b], Juan José Quiroz Ramírez [a,*]

[a] CONAHCyT- CIATEC, Center for Applied Innovation in Competitive Technologies, Mexico
[b] Department of Chemical Engineering University of Guanajuato, Noria Alta S/N, Guanajuato,Gto., 36000, Mexico
[c] Department of Mathematics and Statistical Science University of Idaho, 875 Perimeter Drive, Moscow, MS 1103, USA

ARTICLE INFO

Keywords:
Biojet-fuel
Reactive distillation
Process intensification
ATJ process
Model predictive control

ABSTRACT

Biojet-fuel represents a promising avenue for decreasing CO_2 emissions within the aviation industry. Among different biojet-fuel production processes, the Alcohol-to-Jet (ATJ) process stands out as highly promising. Despite its potential, the ATJ process currently faces economic challenges due to low yields and high energy usage. This study introduces a strategy for enhancing the economic feasibility of the ATJ process through process intensification, specifically by incorporating a novel reactive distillation column in the oligomerization stage. This innovative process was evaluated and compared with its conventional counterpart. The total annual cost, eco-indicator 99, and individual risk were chosen as critical parameters for assessing the improvements in cost, environmental impact, and safety brought about by the reactive column. Additionally, control studies were conducted using both Proportional-Integral (PI) and Model Predictive Control (MPC) controllers to determine the feasibility of operating the reactive distillation column. The results suggest that the reactive distillation process offers 20 % cost savings, reduces environmental impact by 50 %, and lowers risk by 22 % when compared to the conventional process. In terms of control strategies, the study found that the catalytic column can be successfully operated using both traditional feedback control and more advanced techniques, such as model predictive control.

1. Introduction

Energy has a crucial role in society since it is used to produce and provide commodities and services essential for humankind, such as polymers, fertilizers, natural gas, and liquid fuels. Currently, the transportation sector is the largest energy consumer. In the United States alone, the transportation sector represents around 37 % of the country's total energy consumption, which exceeds the energy use of other sectors such as industrial or residential [1]. In addition, it is projected that the energy consumption of this sector will increase up to 130 % by 2050 [2]. Meanwhile, the U.S. Energy Information Administration (EIA) reports that approximately 90 % of the total energy consumption of the transportation sector is derived from fossil sources [1]. This fact, combined with the fast consumption growth, underscores the need to replace fossil fuels with sustainable alternatives to reduce CO_2 emissions. Despite the Covid-19 pandemic, the aviation sector has shown the fastest growth in recent years among all transportation means and is expected to double its size and emissions by 2050, representing a 700 % increase in CO_2 emissions since 2005 according to data presented by the International Air Transport Association (IATA) [2–6]. Accordingly, the IATA has committed to halving the CO_2 emissions of the aviation industry by 2050 [5,6]. To achieve this, the aviation industry has explored alternatives such as reducing fuel consumption by searching for new routes, improving aircraft turbine efficiencies, and developing and using alternative environmentally friendly fuels [6–8]. Among these alternatives, the use of sustainable aviation fuel (SAF), also known as biojet-fuel, is considered the most promising alternative to reduce emissions by the IATA [5,6].

Biojet-fuel is a mixture of hydrocarbons with boiling points between C8 and C16, a range similar to the hydrocarbons found in fossil jet fuel. The main differences between biojet-fuel and fossil jet fuel are the absence of aromatic compounds and lower levels of branched hydrocarbons in biojet-fuel [9,10]. The biojet-fuel can be produced from different sources of biomass, such as lignocellulosic wastes, fatty acids,

* Corresponding author.
E-mail address: jquiroz@ciatec.mx (J.J.Q. Ramírez).

https://doi.org/10.1016/j.cep.2023.109548
Received 12 May 2023; Received in revised form 6 September 2023; Accepted 8 September 2023
Available online 13 September 2023

triglycerides, sugars, wood, and starchy biomasses. However, each type of biomass requires a different process to convert it into SAF. Currently, there are only six certified processes to produce biojet-fuel for commercial flights: Fischer–Tropsch (FT), Hydroprocessed Esters and Fatty Acids (HEFA), Direct Sugars to Hydrocarbons (DSHC), Fischer–Tropsch with Aromatics (FT-SPK/A), Alcohol to Jet (ATJ-SPK), and Co-processing of renewable lipids with crude oil-derived middle distillate [8]. Among all the biojet-fuel routes, the ATJ process is one of the most attractive due to the variety of biomasses and alcohols that can be used to produce jet fuel. Moreover, alcohols are produced in abundance, which offers logistical flexibility.

The ATJ process consists of four steps: alcohol dehydration, olefin oligomerization, hydrogenation, and hydrocarbon separation. Although the ATJ process uses well-established technologies that have been employed for many years in the chemical industry, there are still several challenges to overcome in order to achieve an economically feasible process. According to previous researches, the low conversion yields from biomass to alcohols and the high energy consumption required for alcohol purification are the primary factors that hinder the ATJ process's economic viability [8]. Therefore, it is of utmost importance to develop more efficient bioprocesses for alcohol production. However, it is important to note that alcohol production is not part of the ATJ process. Furthermore, certain stages of the process, such as alcohol dehydration, oligomerization and hydrogenation, have high energy consumption which needs to be decreased to improve the process's economic feasibility [8]. Some studies have focused on improving the dehydration, oligomerization, and hydrogenation stages of the ATJ process through process intensification, heat integration, and the development of new catalysts, among other methods, in order to compensate for the high costs and low yields of alcohol production. Nevertheless, there are limited studies in this area.

Romero-Izquierdo et al. [8] intensified the separation zone of the ATJ process, which consists of several distillation columns. They proposed different thermally coupled arrangements and heat integration configurations to reduce energy consumption, CO_2 emissions, and operational costs. Their results showed that thermally coupled distillation systems could reduce the energy requirements of the ATJ process by only 5 % compared to conventional arrangements. However, energy savings of up to 34.75 % can be achieved when heat integration is applied. Dagle et al. [11] studied the production of different fuels and their properties by controlling the degree of branching of iso-olefins obtained from butene oligomerization. They found that selecting appropriate parameters such as temperature, weight hourly space velocity, nature of butene feedstock, and proper catalyst choice can improve the production of fuels such as gasoline and jet-fuel, which significantly impacts the reduction of separation costs.

Saavedra Lopez et al. [12] reported a solid catalysts based on zeolites and polymeric resins to improve the selectivity of hydrocarbons for fuel production during the oligomerization of propene and isobutene. They found that the H-beta catalyst at 200 °C can produce significant quantities of hydrocarbons in the jet-fuel range. Moreover, these hydrocarbons, with the proper hydrotreating process, can generate jet-fuel that meets ASTM 7566 specification. Brooks et al. [13] studied the oligomerization stage of the ATJ process, which is one of the most crucial parts of the process since this is where the C12 hydrocarbons required for jet-fuel are produced. They examined several processes that use intermediate olefins such as butene, hexene, or polypropylene to produce biojet -fuel. Their results showed that the butene route produces oligomers to C12 more efficiently than other intermediates, with a selectivity of more than 90 %. Additionally, they concluded that future work should focus on quantifying yields, capital and operating requirements, and external energy requirements.

As aforementioned, most of the previous works have focused on intensifying the separation zone and improving the reaction zone through the search for new catalysts or novel chemical routes. However, the possibility of implementing reactive distillation in the oligomerization zone has not been explored to date. Reactive distillation (RD) combines the reaction and separation stages into a single piece of equipment, resulting in several benefits such as lower capital costs, energy savings, and improved safety due to fewer process equipment are required [14,15]. Reactive distillation has been successfully implemented in several processes. A good example of this is the methyl acetate process, which was traditionally performed using a reactor and a set of nine distillation columns. This process was replaced by Eastman Kodak Company with just one reactive distillation column, which achieves near 100 % conversion of the reactants and drastically reduces the operating costs of the process [15]. Another example of successful implementation of reactive distillation in the industry is observed in the production of Methyl tert-butyl ether (MTBE), which is used as an octane booster. The conventional process to produce MTBE consists of a catalytic reactor with an excess of methanol. However, several reactive distillations are required to separate the MBTE-Methanol mixture and the isobutylene-Methanol due to the formation of azeotropes. However, the reactive distillation process only requires one column, achieving complete conversion of methanol and isobutylene while eliminating the azeotropes during the process. The company Chemical Research and Licensing Company is pioneering the commercialization of this technology [16]. Additionally, numerous alkylation reactions, such as aromatic to olefin and alkyl aromatic, are optimally performed using the reactive distillation This is not just because of the reaction equilibrium shift caused by in situ separation, but also because it suppresses unwanted side reactions like alkyl aromatic to olefin and di-alkyl aromatic. An example of this is the reaction between propene and benzene to create cumene [15,17]. Contreras-Zarazua et al. [18,19] proposed several alternative methods for producing Diphenyl Carbonate (DPC) through reactive distillation. These methods include conventional reactive distillation, thermally coupled reactive distillation, and reactive distillation with vapor recompression. Their findings indicated that certain configurations have the potential to reduce total annual cost by up to 50 %. In the case of bio jet fuel production, Gutierrez-Antonio et al. [2] proposed a novel reactive distillation column to enhance the hydrotreating process. This column integrates the hydrocracking and hydro-isomerization stages into a single reactive column, allowing for up to a 25 % reduction in energy and CO_2 emissions compared to the conventional process.

Nonetheless, reactive distillation has drawbacks due to its highly nonlinear behavior, such as multiple steady states, changes in process gain signs (bi-directionality), strong interaction between process variables, and high sensitivity to disturbances on operating variables. These challenges could make reactive distillation columns difficult to control and operate. For these reasons, performing control studies on these processes is of utmost importance [20–22]. In this regard, numerous works have focused on developing, and applying different control strategies to reactive distillation columns; these control strategies range from typical feedback control strategies to advanced predictive control techniques. In this sense, one of the best compilations about control of reactive distillation columns is presented by Luyben [22].

In this work, a novel reactive distillation column was designed for the oligomerization stage of the ATJ process to explore the feasibility of its implementation. The design parameters and operating conditions of the column were selected to maximize the hydrocarbon's the necessary physical properties for jet fuel, as specified by the ASTM D7566-21 standard [23]. To determine the benefits and improvements of the reactive distillation, its economic, environmental, and safety aspects were compared to those of the conventional oligomerization counterpart. The metrics used to quantify these aspects were the total annual cost, Eco-indicator 99, and individual risk, respectively. Owing to the complexity of the novel reactive distillation equipment, a control study was performed in order to determine the feasibility of operation. The control study comprised a comparison of using feedback control techniques using proportional-integral controllers (PI) and model predictive control.

2. Conventional process design and simulation

The ATJ process has the capability to use one or more types of alcohols for biofuel production. However, in this study, it is assumed that the ATJ process only uses ethanol as raw material, since it is the most produced and widely available alcohol. The ethanol is dehydrated to produce ethylene, which is then fed into an oligomerization stage. This stage is crucial in the ATJ process because it produces the necessary hydrocarbon chains (C8-C16) for biojet-fuel, and this stage also requires significant amounts of energy. For these reasons, this study is focused on the oligomerization zone. It is assumed that only ethylene is fed to the oligomerization stage and only linear olefins are produced; this assumption is realistic according to previous studies that used different catalysts [24–26]. Additionally, it is common practice to add an isomerization reactor after hydrogenation or oligomerization stages in order to obtain branched hydrocarbons [27–29]. Both conventional and intensified processes were designed and simulated using Aspen Plus software. The Soave–Redlich–Kwong (SRK) thermodynamic model was employed to simulate the conventional process and the reactive distillation column, since it is suitable for the linear hydrocarbons present in the system and the pressure and temperature conditions required for oligomerization. This thermodynamic approach was selected based on Carlson's algorithm [30].

Fig. 1(a) shows a flowsheet of the oligomerization stage for the ATJ process. Please note that the oligomerization stage consists of three main pieces of equipment: an oligomerization reactor, a distillation column, and a compressor. In this work, it is considered that a mass flowrate of 2100 kg/h of pure ethylene is fed to the oligomerization stage. This feed flowrate was chosen in order to generate 1269 kg/h of SAF, which is equivalent to 10,786.5 tons per year of jet-fuel according to the data presented by Rivas-Iteran et al. [31]. This quantity is proposed in order to satisfy one-fifth of the jet-fuel required at Mexicos City airport each year, which is the largest airport in the country [23]. This ethylene is converted into linear olefins in the oligomerization reactor using a Nickel (II)-Exchanged Silica–Alumina catalyst [32,33]. The reactions that occur with this catalyst, along with their respective rate expressions, are represented in Eqs. (1)–(8) [33]. It's crucial to mention that these reaction rates are measured in units of (kmol/ s·kgcat). This is because they are part of a reaction involving a heterogeneous catalyst [33]. These reactions can be performed at temperatures between 100 and 400 °C and pressures of 1–30 atm [32,34]. The kinetic parameters for these reactions fit the Arrhenius equation and were taken from Sanchez-Ramirez et al. [33]. The kinetic parameters of these reactions are shown in Table 1. As detailed by Heydenrych et al. [32] the oligomerization reactions of ethylene take place in both the vapor and liquid phases. Lighter olefins, such as ethylene and butene, are involved in vapor phase reactions, while olefins heavier than C6 are produced in the liquid phase.

$$2C_2H_4 \xrightarrow{k_1} C_4H_8 \qquad r_1 = k_1 C_{C_2H_4}^2 \qquad \textbf{Gas phase reaction} \tag{1}$$

$$2C_4H_8 \xrightarrow{k_2} C_8H_{16} \qquad r_2 = k_2 C_{C_4H_8}^2 \qquad \textbf{Gas phase reaction} \tag{2}$$

$$C_2H_4 + C_4H_8 \xrightarrow{k_3} C_6H_{12} \qquad r_3 = k_3 C_{C_2H_4} C_{C_4H_8} \qquad \textbf{Gas phase reaction} \tag{3}$$

$$C_2H_4 + C_6H_{12} \xrightarrow{k_4} C_8H_{16} \qquad r_4 = k_4 C_{C_2H_4} C_{C_6H_{12}} \qquad \textbf{Liquid phase reaction} \tag{4}$$

$$C_2H_4 + C_8H_{16} \xrightarrow{k_5} C_{10}H_{20} \qquad r_5 = k_5 C_{C_2H_4} C_{C_8H_{16}} \qquad \textbf{Liquid phase reaction} \tag{5}$$

$$C_2H_4 + C_{10}H_{20} \xrightarrow{k_6} C_{12}H_{24} \qquad r_6 = k_6 C_{C_2H_4} C_{C_{10}H_{20}} \qquad \textbf{Liquid phase reaction} \tag{6}$$

$$C_2H_4 + C_{12}H_{24} \xrightarrow{k_7} C_{14}H_{28} \qquad r_7 = k_7 C_{C_2H_4} C_{C_{12}H_{24}} \qquad \textbf{Liquid phase reaction} \tag{7}$$

$$C_2H_4 + C_{14}H_{28} \xrightarrow{k_8} C_{16}H_{32} \qquad r_8 = k_8 C_{C_2H_4} C_{C_{14}H_{28}} \qquad \textbf{Liquid phase reaction} \tag{8}$$

It is important to note that the reactions involved occur in a sequential manner (a set of series reactions), making residence time crucial for producing the desired olefins. The oligomerization reactor was designed as an isothermal tubular reactor (PFR block), based on the methodology presented by Fogler [35] for handling complex reactions. In this sense, according to Yang et al. [36], hydrocarbons ranged between C10 and C16 are usually the most abundant compounds in biojet fuel, and consequently, the properties of jet fuel depend largely on these compounds. As such, the reactor volume was chosen to maximize the production of C10-C16 alkenes to obtain a hydrocarbon distribution that can meet the biojet-fuel specifications according to ASTM D7566-21. This standard specifies that biojet-fuel produced *via* the ATJ process must have a boiling point ranging from 205 to 300 °C at atmospheric pressure and a density between 730 and 770 kg/m^3 at 15 °C [23]. To evaluate the mixture's properties, a stoichiometric reactor and two heat exchangers were used. The stoichiometric reactor is employed to hydrogenate the oligomerization products, and the heat exchangers are used to calculate the boiling point temperatures and densities. Please note that these pieces of equipment were only used to verify the properties of the mixture; therefore, they are not included in the process flow diagram. The flowsheet used to test the properties is shown in Fig. S1 of the supplementary material.

After the olefins are produced, the lighter olefins are separated from the heavier ones (C6-C16) using a conventional distillation column with a partial condenser. The light olefins are recovered as vapor at the top of the column and sent to a compressor, which increases their pressure before recycling them to the oligomerization reactor. The heavier olefins are removed from the bottom of the column. The number of trays in this column was calculated using the DSTW block. Once the number of trays and the feed tray of the column were determined, the RADFRAC block was employed to simulate it rigorously.

3. Design and simulation of the reactive distillation column

The intensification of the oligomerization zone was carried out through reactive distillation specifically a catalytic reactive distillation column. The term 'catalytic distillation' is applied for such reactive distillation systems where a heterogeneous catalyst is used to accelerate

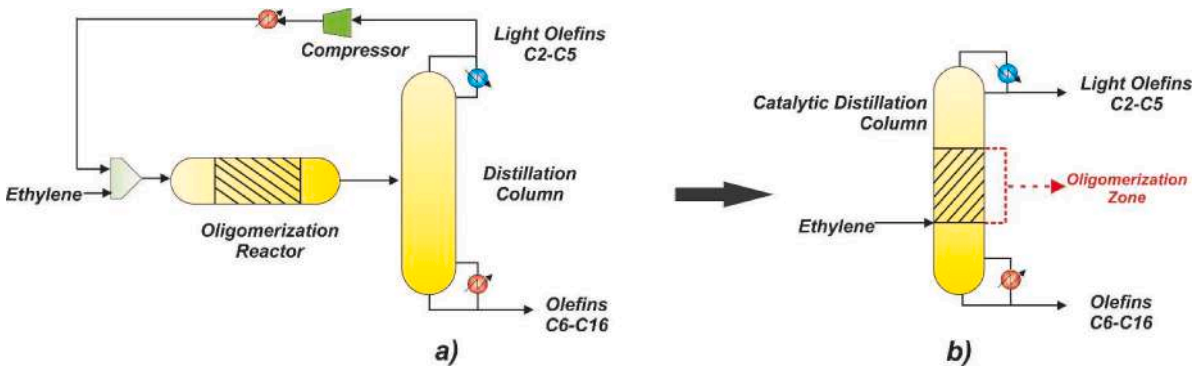

Fig. 1. (a) Conventional oligomerization process (b) Intensification of oligomerization zone using a catalytic reactive distillation column.

Table 1
Reactions and reaction rates expressions for the oligomerization of ethylene using Nickel (II)-Exchanged Silica–Alumina Catalyst [33].

Reaction Number	Pre-exponential factor	Activation energy (kJ/kmol)
Reaction 1	38,728.6	4.62
Reaction 2	3349.12	158.53
Reaction 3	74,825.7	14.93
Reaction 4	48,935.42	164.88
Reaction 5	110,614.01	16.21
Reaction 6	83,400.86	17.50
Reaction 7	116,517.95	21.47
Reaction 8	27,140.87	19.76

the reaction. Fig. 1(b) shows the scheme of the intensified reactive distillation column. This reactive column consists of an intermediate reactive zone where the catalyst is located and the entire set of reactions takes place. Below and above this reaction zone are located separation stages, which are responsible for separating the light and heavy olefins. Please note in Fig. 1(b) that the light olefins are removed from the top of the column whereas the heavy olefins (C6-C8) are removed from the bottoms.

The reactive distillation column was designed and simulated using the RADFRAC module, which includes and solves the comprehensive set of MESH equations. As in the conventional process, the design of the reactive distillation column aimed to achieve an appropriate hydrocarbon distribution of olefins at the column's bottom in order to ensure suitable physiochemical properties for bio jet fuel [37]. The Soave–Redlich–Kwong (SRK) thermodynamic model was used to simulate the column, chosen based on Carlson's algorithm [30].

The design of a reactive distillation column involves numerous variables, such as the total number of trays, feed tray location, reflux ratio, reboiler duty, and reactive stage hold-up. All these variables must be synergized to achieve the desired hydrocarbon distribution. Given the column's complexity and large number of variables involved, there is no general design method for reactive columns. Although some previous works have discussed simultaneous design and optimization techniques for reactive distillation columns, these methods are not considered proper design techniques [16,36]. Additionally, these approaches require complex mathematical optimization techniques, lengthy computational times, and a preliminary design of the reactive equipment before initializing the algorithm. Consequently, these strategies may not be ideal for easily exploring process intensification feasibility, especially during the early stages. Therefore, this work assesses the feasibility of an intensified process for the oligomerization zone using reactive distillation by designing the intensified equipment through a sensitivity analysis. It is worth noting that sensitivity analysis has been employed in previous studies for the design of reactive distillation columns [22,38,39]. The design variables for the catalytic column include the total number of stages, feed tray location, and reactive stages, while the operative variables encompass the reflux ratio, reboiler duty, and liquid and vapor hold-ups. As a result, there are six degrees of freedom that can be manipulated to achieve a suitable design. The steps and procedures used to generate the catalytic column design are as follows:

1 Guess the total number of stages (NS_i) for the catalytic column.
2 Guess the ethylene feed stage location (FS_i).
3 Guess the liquid hold-up.
4 Vary the vapor hold-up.
5 Adjust the reflux ratio and reboiler duty to obtain a hydrocarbon distribution similar to that reported by Li et al. [37].
6 Return to step 3 and repeat steps 4 and 5.
7 Return to step 2 and repeat steps 3, 5, and 6 until obtaining a suitable hydrocarbon distribution and minimum reboiler duty.
8 Return to step 1 and repeat the entire procedure until maximizing the production of C12.

4. Performance criteria

In this section, the indices used to compare the conventional and intensified oligomerization processes are explained. As previously mentioned, the total annual cost, eco-indicator 99, and individual risk are the metrics used to evaluate the economic, environmental, and safety aspects of the processes. These criteria were selected in accordance with the twelve principles of green and sustainable processes proposed by Jiménez-González and Constable [40] which chemical processes must fulfill.

4.1. Total Annual Cost (TAC)

The Total Annual Cost (TAC) is a common metric employed to assess the economic performance of different chemical process options. TAC includes the sum of the annualized capital cost and operating cost. Capital costs involve expenses related to constructing process equipment, including condensers, reboilers, distillation columns, trays, process vessels, and compressors. On the other hand, operating costs encompass expenses for electricity, cooling water, steam, among others. Mathematically, TAC can be expressed as follows:

$$\text{TAC} = \frac{\text{Capital cost}}{\text{Payback period}} + \text{Operating cost} \tag{9}$$

Carbon steel was the construction material considered, and a payback period of ten years was considered. The TAC was calculated by the Guthrie's method and using the parameters and equations reported by Turton et al. [41]. Sieve-type trays with 0.61 m spacing were considered for distillation columns. The utilities costs were calculated considering 8500 h of operation per year. The utilities used in this study and their respective cost are: low-pressure steam (160 °C, $14.05/GJ), medium-pressure steam (184 °C, $14.83/GJ), high-pressure steam (254 °C, $17.7/GJ), Fire heat (300 °C, $20.92/GJ) cooling water ($0.354/GJ) and electricity ($16.8/GJ) [41]. For further details, the

complete model for TAC calculation and the set of correlations used in this work are provided in the supplementary material.

4.2. Eco-Indicator 99 (EI99)

The Eco-Indicator 99 was the method used to quantify the environmental impact of the processes. It is a life cycle assessment method proposed by Goedkoop and Spriensma [42]. This method has been successfully implemented in previous studies to evaluate and compare the environmental impact of different technologies [43,44]. The EI99 evaluates multiple environmental impact areas grouped into three primary categories: ecosystem quality, resource depletion, and human health. These categories are further divided into eleven sub-categories, including climate change, ozone depletion, human toxicity, ecotoxicity, respiratory effects, land acidification, land occupation, fossil fuels, mineral extraction, and others. It assigns impact scores to different activities or processes involved in the life cycle of a product or service, such as raw material extraction, manufacturing, transportation, use, and disposal. The scores provided by the Eco-Indicator 99 are expressed in "eco-points," where a higher score indicates a greater potential environmental impact. Each point is associated with the 1000th part of the environmental load of one average European inhabitant per year [42]. This method allows for the comparison of different products or services and helps identify areas where improvements can be made to reduce environmental burdens.

It is worth emphasizing that the Eco-Indicator 99 methodology employs an impact assessment approach. This approach involves multiplying the inventory data (such as quantities of energy, water, and emissions associated with a process) by their corresponding characterization factors (C_i). Previous studies have identified that the most significant environmental contributions in a chemical process are attributable to the steam used for energy, the electricity needed for operating cooling utilities, and the steel employed in equipment construction [45,46]. Consequently, the data presented in Table 2 correspond to the characterization factors for the different impact categories related to energy, electricity, and steam. The equation used to calculate the Eco-Indicator 99 is expressed as follows:

$$EI99 = \sum_i \omega \cdot c_i \cdot as + \sum_i \omega \cdot c_i \cdot ast + \sum_i \omega \cdot c_i \cdot ae \tag{10}$$

In the given context, the weighting factor for damage is denoted as ω. C_i is the characterization factor for a specific category i. Additionally, *as* represents the amount of steam used by the process, *ast* represents the amount of steel utilized in constructing the equipment, and *ael* corresponds to the electricity required by the process. It is important to note that the weighting factor ω represent the importance given to the environmental effects originating from the process in the short, medium, and long term [47]. In this work, a hierarchical approach was used to balance both short-term and long-term environmental impacts. Consequently, the weighting factors for major impact categories, such as human health, ecosystem quality, and resource depletion, were determined based on the hierarchical analysis outlined by Errico et al. [45] and Cheng et al. [39]. Therefore, damages to human health and ecosystem are assigned equal importance and weighting, while resource-related damages receive half the importance.

Table 2
Characterization factors (C_i) for the different impact categories to for energy, the electricity and steam (Heydenrych et al. [32]).

Impact category	Steel (points/kg) × 10^{-3}	Steam (points/kg)	Electricity (points/kWh)
Carcinogenic	1.29×10^{-3}	1.180×10^{-4}	4.360×10^{-4}
Climate change	1.31×10^{-2}	1.27×10^{-3}	4.07×10^{-3}
Ionizing radiation	4.510×10^{-4}	1.91×10^{-6}	8.94×10^{-5}
Ozone depletion	4.550×10^{-6}	7.78×10^{-7}	5.41×10^{-7}
Respiratory effects	8.010×10^{-2}	1.56×10^{-3}	1.01×10^{-5}
Acidification	2.710×10^{-3}	1.21×10^{-4}	9.88×10^{-4}
Ecotoxicity	7.450×10^{-2}	2.85×10^{-4}	2.14×10^{-4}
Land occupation	3.730×10^{-3}	8.60×10^{-5}	4.64×10^{-4}
Fossil fuels	5.930×10^{-2}	1.24×10^{-2}	1.01×10^{-2}
Mineral extraction	7.420×10^{-2}	8.87×10^{-6}	5.85×10^{-5}

4.3. Individual Risk (IR)

The metric chosen for safety assessment is the Individual Risk (IR), which represents the probability of a person to be affected by an accident. IR is independent of the number of people exposed, since it measures the likelihood of damage based on the distance between the accident's epicenter and the individual's location. Mathematically, the individual risk can be expressed using the following equation:

$$IR = \sum f_i P_{x,y} \tag{11}$$

where, f_i is the occurrence frequency of incident i, whereas $P_{x,y}$ is the probability of affectation caused by the incident i. IR is calculated using Quantitative Risk Analysis (QRA), which is a method that quantifies potential incidents and their consequences. Incidents are categorized into continuous releases, caused by ruptures in pipelines or process equipment, and instantaneous releases, resulting from catastrophic equipment failures. A Hazard and Operability study (HAZOP) was employed to identify potential incidents. The incidents identified by the HAZOP and their respective frequencies are shown in Fig. S2 of supplementary material

The probability of damage, $P_{x,y}$, is determined by calculating the physical variables (e.g., thermal radiation, overpressure, leak concentration) and their respective damages for each incident. The equations used to calculate the physical variables of each incident are reported by CCPS [48]. A probit model is used to relate these physical variables to the damage caused to a person, with death being the considered damage [48]. The Probit models associated with deceases by thermal radiation ($t_e E_r$) and overpressure (p°) are given due to explosions are provided in Eq. (12) and Eq. (13), respectively.

$$Y = -14.9 + 2.56 \ln\left(\frac{t_e E_r^{\frac{4}{3}}}{10^4}\right) \tag{12}$$

$$Y = -77.1 + 6.91 \ln(p^\circ) \tag{13}$$

where, Y (dimensionless) is the probit variable, t_e (s) represents the exposure time, E_r (W/m2) is the thermal radiation emitted by a fire or explosion, and p° (Pa) is the overpressure generated by an unconfined vapor cloud explosion (UCVE). It is crucial to mention that all calculations were performed based on a representative distance of 50 m. The probability ($P_{x,y}$) which is computed by the substitution of probit equations Eqs. (12) and (13) into the following equation:

$$P_{x,y} = 0.5\left[1 + erf\left(\frac{Y-5}{\sqrt{2}}\right)\right] \tag{14}$$

For toxic releases, the probability ($P_{x,y}$) is determined using the LC50 (Lethal median concentration), since there is a lack of probit models for toxic releases of different substances. To calculate the concentrations of chemical compounds during a toxic release incident, an atmospheric stability type F with a wind speed of 1.5 m/s is assumed, representing the worst-case scenario according to Crowl and Louvar [49]. The physical properties of each substance used in the consequence assessment can be found in Table 3. Additionally, the complete set of equations employed to calculate the physical variables, such as the concentration of toxic substances (C), thermal radiation (E_r), and overpressure (p°), is shown in the supplementary material. This is due to the complexity and large number of equations required. Finally, it is important to note that the properties listed in Table 3 are used in those

Table 3
Physical properties of compounds.

Component	Molecular weight (gr/mol)	Lower flammability limit (LFL)	Upper flammability limit (UFL)	Median lethal concentration (rat) (LC50)/1h	Heat Combustion (kJ/kg)
Ethylene	28.05	2.7	28.6	2362	50,303
1-Butene	56.108	1.6	10	1032,000	44,911
1-Hexene	84.16	1.2	9	128,000	44,343
1-Octene	112.24	0.9	8	32,200	44,202
1-Decene	140.27	0.9	7	12,000	47,191
1-Dodecene	168.32	0.6	5.4	10,000	43,687
1-Tetradecene	196.37	0.3	4	13,900	40,940
1-Hexadecene	224.43	0.5	5.8	8500	46,959.96

equations.

5. Control study of reactive distillation column

Reactive distillation columns are complex and exhibit highly non-linear behavior, which can make them difficult to control and operate. To determine the operational feasibility of the catalytic distillation column, a two-part control study was performed. The first part involves the use of integral proportional controllers (PI), which are commonly used in the chemical industry. The second part explores the feasibility and potential benefits of implementing model predictive control (MPC) techniques. The study aims to evaluate if the column can be operated using typical control strategies (PI controllers) and assess the advantages of predictive control systems in reactive distillation columns. The control study simulates unmeasurable disturbances through changes in ethylene feed and other manipulate variables by applying both positive and negative disturbances of 1 and 5 %. The integral absolute error (IAE) is used as a metric to compare the closed-loop performance of both PI and MPC controllers, this index is defined as follows:

$$\text{IntegralofAbsuloteError(IAE)} = \int_0^\infty \left| y(t) - y_{sp} \right| dt \tag{15}$$

where, y_{sp} is the value of the set point for control variables, whereas $y(t)$ is the value of control variable at any the time.

5.1. Control using proportional-integral controllers

The first part of the control study focuses on using proportional integral controllers for the reactive distillation column. It was done using Aspen Dynamics software for dynamic simulations. In order to export the Aspen Plus simulation to Aspen Dynamics, a pressure drop of 0.0068 atm per tray (0.1 psi per tray) was considered. This pressure drop was also taken into account for the reactive stages due to the lack of information about the hydraulics of the catalyst. However, it is important to note that this pressure drop is considered reasonable and suitable based on the information reported by Luyben [22] and Luyben [50]. A typical L-V control structure was chosen, it consists of feedback control scheme that involves controlling the purity of the bottom stream with reboiler duty and the top stream with reflux ratio [51,52]. In addition, this arrangement is one of the most used by the industry and has been tested successfully in different reactive distillation columns, including a reactive distillation column to produce light olefins [38,53]. Fig. 2(a) shows the control scheme for the reactive distillation column. It is important to highlight, that the most abundant compound in each stream was used as a control variable. The PI controller's parameters, gain (Kc) and integral time (τi), were tuned by minimizing the IAE, as shown in Fig. 2(b). The tuning was conducted within the range of industrial values reported by Luyben [22], and each controller was tuned separately.

5.2. Control using model predictive controllers

The second part of the control study employs model predictive control techniques. In recent years, model predictive control (MPC) has become increasingly popular and is on track to be a new industry standard. MPC offers benefits over traditional control methods, such as anticipating future events and improving safety, as well as reducing stabilization time during disturbances, leading to better product quality [44]. MPC is based on a multivariable optimization control problem, therefore, it requires a mathematical model coupled to real-time process information to predict and optimize future responses [54–57]. In this work, a state space (SS) model, which is a linear time-invariant model, was used to approximate the nonlinear behavior of the process near its nominal operation point. Mathematically, the state model can be described as follows:

$$\dot{x}(k) = Ax(k) + Bu(k) \tag{16}$$

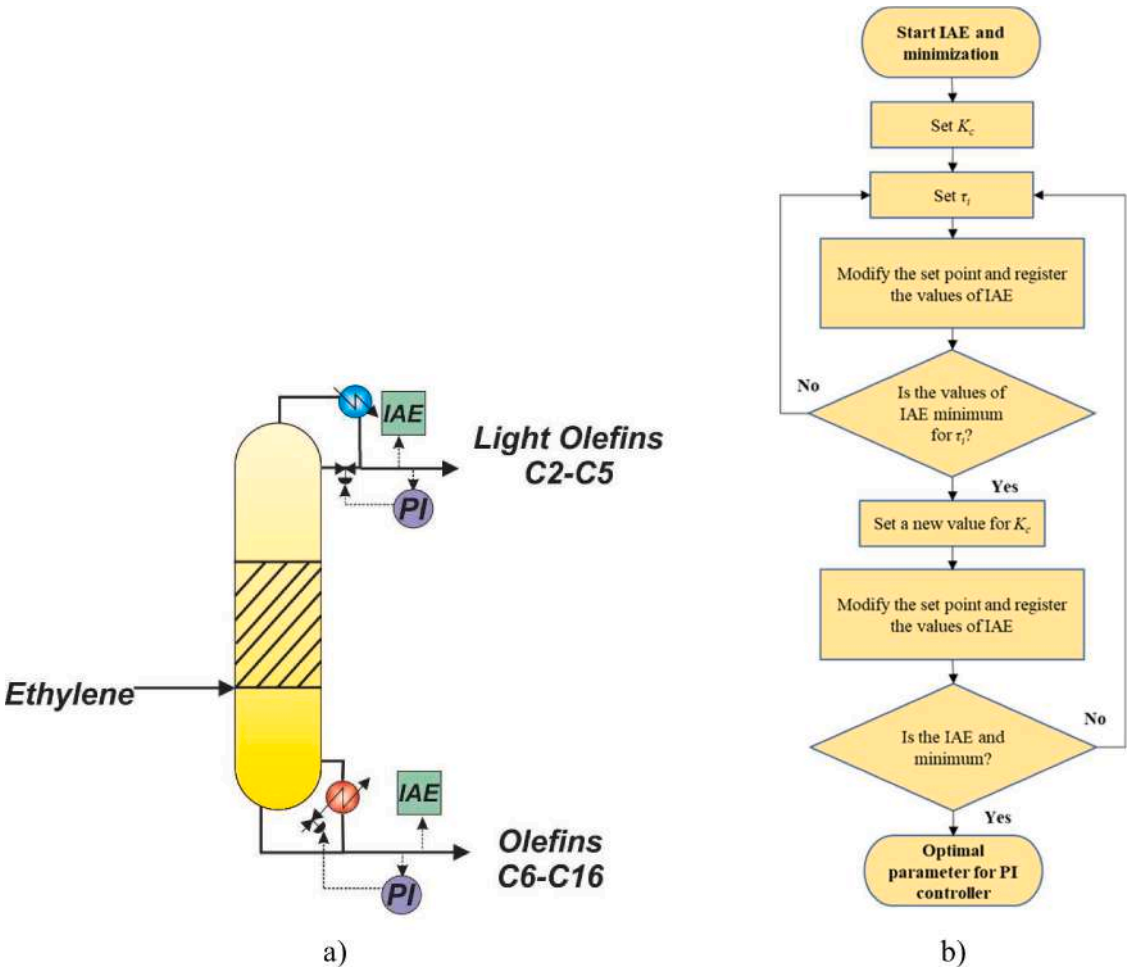

Fig. 2. (a) Control scheme using PI controllers (b) Flowchart of the tuning procedure for PI controllers.

$$y(k) = Cx(k) + Dd(k) \tag{17}$$

where, *x(k)* represents the plant states, *y(k)* is the vector of controlled variables, *u(k)* indicates the vector of manipulated variables, and *d(k)* is the vector of disturbances. Furthermore, *A, B, C*, and *D* are the model matrices that can be obtained by linearizing the nonlinear plant model or through system identification.

The model of the catalytic column is very complex, since it integrates the reaction stage, which contains several chemical reactions, and the separation stage in a single unit. Consequently, linearizing of this highly nonlinear model is not trivial. Therefore, the state space model was obtained using the subspace identification method (system identification), a technique suitable for complex processes. This approach is a common method used to obtain a dynamic model when the process is very complex [58–60]. For this study, the dynamic data were obtained from Aspen Dynamics, where random step changes were made to the manipulate variables. The identification of the dynamic model was performed using deviation variables because most oscillations of a control variable in a real process oscillate around the nominal operating point [58]. In addition, the use of deviation variables or scaled variables makes model identification simpler than employing full-scale variables [59]. The input variables (manipulated variables) used to identify the dynamics are reboiler and condenser duty, reflux rate, and ethylene feed, which is considered, at the same time, as a measured disturbance. Meanwhile, the output variables involved butene composition in the top stream, dodecane (C12) composition in the bottom stream, and pressure at the column top. The input-output data were imported into Matlab's System Identification toolbox, where the data were processed, analyzed, and the identified model was obtained.

The state space model obtained through system identification serves as the predictor model for the MPC controller. With the predictor model established, the next step is to implement and design the predictive controller. This requires formulating an optimization problem that must be solved at each control interval to determine the optimal adjustments for the control variables. The proposed optimization problem consists of a quadratic function (QP). The mathematical representation of the optimization problem is as follows:

$$\begin{aligned}\min J = &\overbrace{\sum_{j=1}^{n_y}\sum_{i=1}^{p}\left(\frac{w_{i,j}}{s_j^y}\cdot\left[r_j(k+i|k) - y_j(k+i|k)\right]\right)^2}^{OutputReferenceTracking} \\ &+ \overbrace{\sum_{j=1}^{n_u}\sum_{i=0}^{p-1}\left(\frac{w_{i,j}^u}{s_j^u}\cdot\left[u_j(k+i|k) - u_{j,target}(k+i|k)\right]\right)^2}^{ManipulatedVariableTracking} \\ &+ \overbrace{\sum_{j=1}^{n_u}\sum_{i=0}^{p-1}\left(\frac{w_{i,j}^{\Delta u}}{s_j^u}\cdot\left[u_j(k+i|k) - u_j(k+i|k)\right]\right)^2}^{ManipulatedVariableMoveSuppression}\end{aligned} \tag{18}$$

Subjet to:

$$\frac{u_{j,\min}(i)}{s_j^u} \le \frac{u_j(k+i|k-1|k)}{s_j^u} \le \frac{u_{j,\max}(i)}{s_j^u}$$

where, n_y is the current number of output plant variables, n_u represents number of manipulated variables, p is the prediction horizon, k is the current control interval $y_j(k+i|k)$ corresponds to the predicted value

for the output plant j at i prediction horizon step, $r_j(k+i|k)$ is the reference value of output j at i prediction horizon state, s_j^y is the scale factor j plant output, in engineering units, $w_{i,j}^y$, $w_{i,j}^u$, $w_{i,j}^{\Delta u}$ are the tuning weights for the j manipulate variable movement at i prediction horizon step (dimensionless). $u_{j,target}(k+i|k)$ is the target value for j MV at prediction horizon step, $u_jt(k+i|k)$ is the output value of process. $u_{j,\min}(i)$, $u_{j,\max}(i)$ are the lower and upper bounds for j MV at i prediction horizon step, in engineering units, in this case the manipulate variables were constrained to be between 20 and 80 % of their minimum and maximum capacity, in order to avoid oversaturation of the control action.

The mathematical model of the controller, which includes both the state space predictor model and quadratic optimization problem, was implemented in Matlab. On the other hand, the Aspen Dynamic model was used as the plant model. The programs were linked through Simulink's AM simulation block, which enables advanced control strategies. The MPC controller model was imported into Simulink using the MPC toolbox, and the IAE calculation for tunning MPC controller was implemented in Simulink. The control scheme using a model predictive controller is shown in Fig. 3. The simulation scheme in Simulink for the model predictive control can be found in the Fig. S3 of the supplementary material. The predictive controller parameters weights ($w_{i,j}^y$, $w_{i,j}^u$, $w_{i,j}^{\Delta u}$), were adjusted to minimize the IAE value of the sum of bottom and top streams, like in the feedback control using PI controllers.

6. Results

This section presents the design and control results of the reactive column and conventional process. This section is organized into two subsections. The first part focuses on the comparison of the reactive distillation column with the conventional process, while the second part is focused on the control results of the reactive distillation column.

6.1. Reactive distillation design results and comparative to conventional process

As mentioned above, both the design of the conventional process and the reactive distillation process were carried out to achieve the physicochemical properties required by the jet-fuel according to the ASTM D7566-21 standard [23]. Due to the wide range of compositions capable of meeting this specification, a hydrocarbon distribution is considered suitable when the hydrocarbons meet the ASTM D7566-21 standard, which establishes that biojet fuel produced *via* the ATJ process must have a boiling point ranging from 205 to 300 °C at atmospheric pressure and a density between 730 and 770 kg/m^3 at 15 °C. Fig. 4 shows the design results for the oligomerization reactor. Additionally, the design specifications for the column, compressor and reactor are shown in Table 4. It is important to note that initially, a sensitivity analysis was performed to determine a suitable temperature that benefits the production of C12 and other hydrocarbons such as C10 and C14. As can be seen in Fig. 4, the production of C12 slightly decreases at higher temperatures. This is beneficial for energy consumption, as it suggests that the oligomerization of ethylene is more efficient at temperatures around 100–200 °C [61]. In this case, a temperature of 200 °C was selected for operating the reactor to ensure the gas-phase reaction of the reactant mixture along the reactor. Please note that this process is selective to C6, as can be explained by referring to Table 1. The results align with previous studies, highlighting two reasons for the low yield of heavier hydrocarbons. The first reason is related to the activation energy. As shown in Table 1, reactions 2 and 4, which correspond to C8 formation, these set of reaction have the highest activation energy and the lowest pre-exponential constants. This suggests that C8 is the most challenging compound to produce as it requires the most energy, thereby serving as the limiting step for the production of C12 and heavier hydrocarbons. The second reason is inherent to the oligomerization process. According to numerous studies, the degree of polymerization, or the formation of heavier hydrocarbons, greatly depends on the concentration of ethylene. Higher concentrations of ethylene favor the formation of lower molecular weight hydrocarbons since the chances of propagation reactions, which produce larger hydrocarbons, are diminished. Once ethylene is depleted, a mixture rich in low molecular weight hydrocarbons is left. The attempt to oligomerize these into larger chains encounters a similar effect to that with ethylene, where high concentrations limit the production of larger hydrocarbons. The formation of higher molecular weight hydrocarbons is further hindered due to the discrepancy in reaction temperatures. Higher temperatures are needed to produce heavier hydrocarbons [28,61,62]. These limitations provoke the recycling heavy hydrocarbons back to the reactor to boost propagation reactions and enhance the production of heavier olefins.

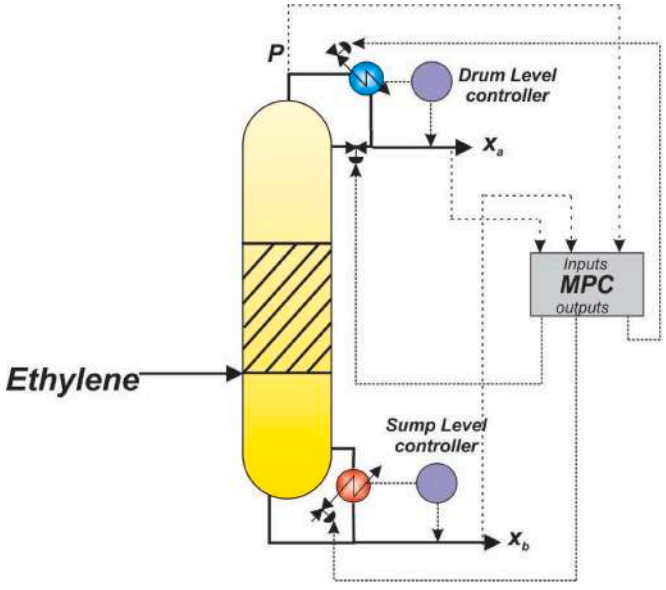

Fig. 3. Control scheme using model predictive control.

These drawbacks of the oligomerization reaction can be overcome using reactive distillation since it facilitates the continuous removal of ethylene from the reaction environment, thus encouraging propagation reactions. Furthermore, the variation in temperature at each stage promotes the formation of heavier olefins as can be observed in Table 5 which shows the design parameters selected for the reactive distillation column obtained by the sensitivity analysis and the compositions obtained. It should be noted that the reactive distillation column should be operated at 15 atm, which is higher than the conventional process, in order to ensure that the reactions are mainly performed in the liquid phase, which is essential for a reactive distillation process. In this work, designs for 20, 30, and 40 stages were studied for the column. The results of the sensitivity analysis are shown in Fig. 5. As aforementioned, the findings indicate that continuous product removal from the reaction medium, coupled with temperature gradients and internal recirculation due to the reflux and boil-up ratios, notably increase the production of heavier hydrocarbons. According to previous studies the biojet-fuel consists of a mixture of hydrocarbons ranged between C8- C16 where the most abundant are the C12 which provides the major properties to bio-jet fuel [63]. In the case of the conventional process, the properties obtained after hydrogenation of the oligomerization products were a boiling point of 121 °C and a density of 730 kg/m^3. This boiling point indicates that the oligomerization products cannot be directly converted into bio-jet fuel. After hydrogenation, the appropriate fractions of hydrocarbons that meet the desired properties (C8-C16 hydrocarbons) need to be purified. This suggests that only a small percentage of the hydrocarbons produced by the conventional process is suitable for bio-jet fuel. On the contrary, the properties obtained after hydrogenating the products of oligomerization in the reactive distillation process

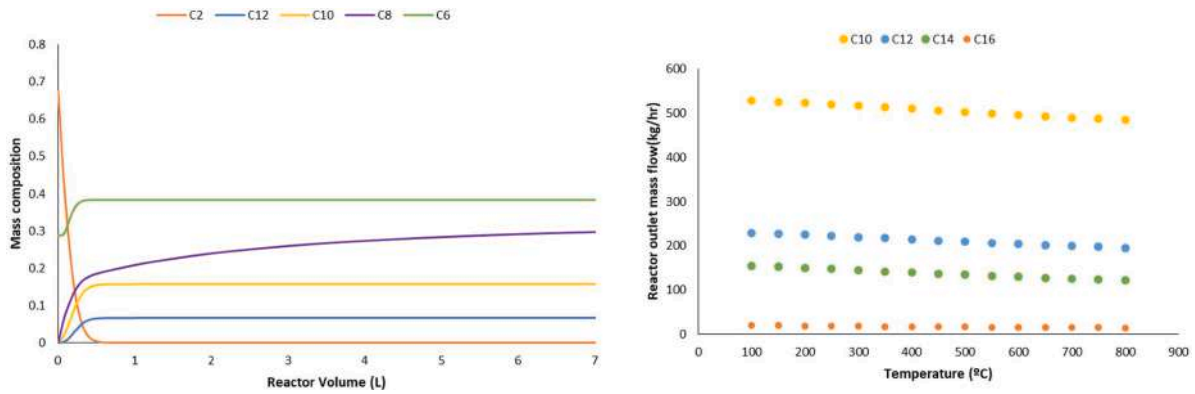

Fig. 4. Effect of the temperature and reactor volume on production of C12.

Table 4
Design parameter for the conventional oligomerization process.

Design parameter	Value
Reactor volume (l)	7
Reactor temperature (°C)	209
Reactor pressure (atm)	3
Reactor energy (kW)	−1682
Colum stages	35
Feed stage	17
Reflux ratio	3.43
Condenser duty (kW)	−349
Reboiler duty (kW)	399.61
Top mass flowrate stream (kg/hr)	1088
Bottoms mass flowrate (kg/hr)	2243.33
Temperature at top of the column (°C)	64.06
Temperature at bottoms of the column (°C)	123.99
Mass fraction at top of the distillation column [C6]	0.9999
Mass fractions at bottom of the distillation column [C6,C8,C10,C12,C14,C16]	[0.074, 0.493, 0.242, 0.11, 0.073, 0.009]
Compressor energy (kW)	28.77
Heat exchanger energy (kW)	−136.63
Heat exchanger temperature (°C)	200

Table 5
Design parameter of oligomerization catalytic column.

Design parameter	Value
Stages	30
Feed stage	8
Reactive stages	2–7
Reflux ratio	40
Reboiler duty (kW)	200
Liquid hold-up (liters)	0.5
Vapor hold-up (liters)	1
Temperature at top (°C)	92.2
Temperature at bottom (°C)	362.3
Distillate flow (kg/h)	546.27
Bottom flow (kg/h)	1697
Mass fraction at top of the column [C4, C6]	[0.94, 0.06]
Mass fractions at bottom of the column [C10,C12,C14, C16]	[0.241, 0.443, 0.267, 0.049]
Ethylene feed flow (kg/h)	2243.25

(bottom products) resulted in a boiling point of 208 °C and a density of 745 kg/m^3. This indicates that the hydrocarbons obtained in the reactive distillation process can be directly used to produce bio-jet fuel without undergoing a fractionation stage, reducing downstream process costs.

Based on the sensitivity analysis results, it was observed that the boil-up play a crucial role in determining the type of hydrocarbon that will be produced. For example, the reboiler duty load has a strong direct, effect on the production of C10, C12, and C14, increasing the production of heavier olefins for larger thermal loads. Based on these results, it is concluded that a reboiler duty of 200 kW is the most suitable for three main reasons: First, there is a satisfactory distribution of hydrocarbons. Second, it represents one of the lowest energy consumption levels at which the reaction can occur. Finally, lower energy consumption and temperatures improve the control of the reaction, as the oligomerization is an exothermic reaction.

Lower reflux ratios have a positive effect on the production of C10 and C12, resulting in a maximum mass flow rate of C12 at values close to 40. For this reason, this value was selected. In terms of the feed stage, it was found that for feed stages lower than 15, the mass flows of C10, C12, and C14 in the bottom stream remain constant. C12 and C14 reach their maximum flows while C10 flows are minimized. Based on these findings, stage 7 is considered the optimal choice as it ensures high mass flow rates of C12 and favorable production of C10 and C14, leading to a satisfactory distribution of hydrocarbons at this stage.

Regarding the reactive stages, when the number of reactive stages exceeds tray 7, the flows of all compounds in the bottom of the column remain constant. As a result, it is determined that the catalytic distillation column should comprise 6 reactive stages, ranging from tray 2 to tray 7. It is important to note that the reactive stages graph represents the final stage of the reactive zone, assuming that the reactive zone starts at stage 2 (the first tray of the column) and concludes at stage 7. It is worth noting that in this case, the reactive zone is situated near the top of the column due to the exothermic nature of the reaction, resulting in lower temperatures in this region. This positioning facilitates better control of the reaction. Consequently, the condenser duty directly affects the production of heavy olefins exiting the column through the bottoms. Based on the results, it was concluded that a column with 20 stages is suitable for achieving the desired distribution of olefins. This determination arises from the observation that the production of C12 does not vary significantly with additional stages. The final design parameters of the catalytic column obtained from the sensitivity study are presented in Table 5. Finally, the olefins distribution obtained with this design (refer to the lower right plot of Fig. 5) closely resembles that reported by Li et al. [37].

So far, it has been demonstrated that the oligomerization stage of the ATJ process can be intensified using reactive distillation. This intensification brings benefits in the form of cost reduction, lower environmental impact, and improved safety, which were measured using the total annual cost, eco-indicator 99, and individual risk, respectively. Fig. 6 presents the results comparing the conventional and intensified processes under these three indicators. The results showed that the reactive column has significant cost savings compared to the conventional process. These savings originate from reduced utility costs, such as cooling water usage, electricity for pumping and compression, and overall energy consumption. It is important to note that, in order to obtain larger chain hydrocarbons, the conventional process necessarily requires a separation stage to recycle part of the hydrocarbons back into the process. This increases the number of equipment and energy

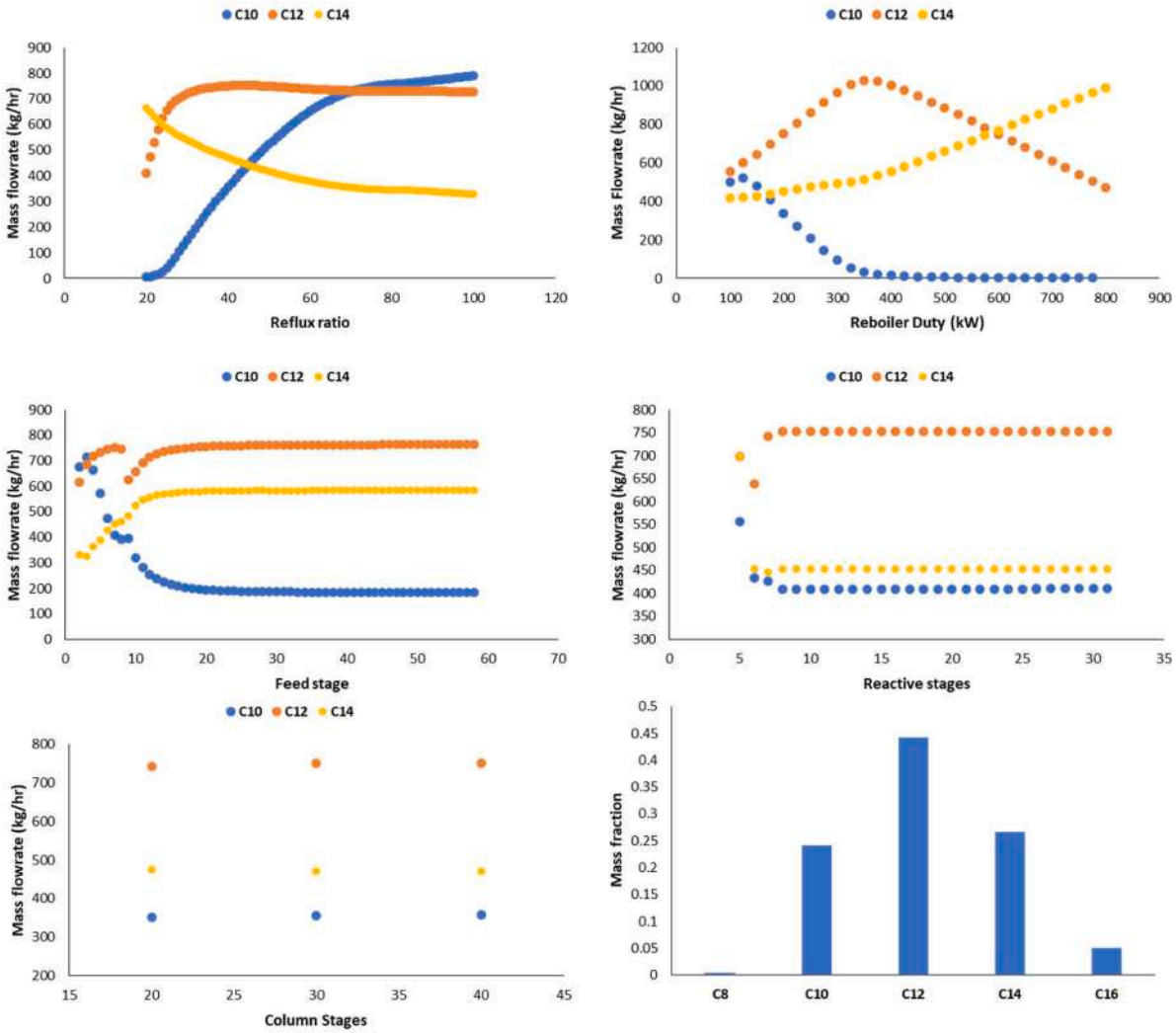

Fig. 5. Design results of catalytic distillation.

required by the conventional process. Additionally, it is noteworthy that the cost of the reactive distillation column alone is higher compared to the conventional process. This is due to the requirement of higher pressure in the reactive distillation column, resulting in the need for more expensive equipment.

In terms of environmental impact, the intensified process has a smaller eco-indicator, indicating a lesser environmental impact. These improvements in environmental impact are associated with the reduced use of energy and electricity for pumping and compression. Considering these factors, the intensified process has 40 % and 60 % fewer eco-points when using electricity and steam, respectively. Among the main factors considered in the environmental study, the use of steel has the least environmental impact, in contrast to the effect associated with the use of steam and electricity. The results indicate a clear relationship between the EI99 and TAC to energy consumption, with this being the factor that contributes most to increasing the cost and environmental impact.

It is important to emphasize that the results presented for both the total annual cost and the Eco-Indicator 99 are based on the assumption that all energy supplied to the process comes from fossil sources, such as natural gas. This represents the worst case from both economic and environmental point of view. However, these "worst-cases" scenarios are typically useful and simplify comparisons between different technologies [64]. It's important to bear in mind that the ATJ process converts lignocellulosic residues into ethanol and then into biojet-fuel. If some fractions of the biomass, such as the lignin, are used to supply energy to the process, both utility costs and environmental impacts from steam use would decrease. Similarly, the consumption of electricity or steam could be further reduced by implementing green technologies based on solar energy, or through heat and energy integration. While this study does not account for the use of green energy sources, it is worth mentioning that the environmental impact of the reactive distillation column would still be less, even with green energy use. This is primarily because this process consumes less energy than its traditional counterpart. Taking these factors into account, we believe that emerging biorefineries, focusing on biofuel production, should incorporate technologies that decrease both costs and environmental impact.

In the case of individual risk, this index indicates that the intensified process is safer than its conventional counterpart, reducing the accident risk by up to 22 %. Key factors contributing to the individual risk index include the quantity of equipment, flammable compound concentrations, and operating conditions like pressure and temperature. The safety improvements of intensified process can be attributed to using less equipment for the oligomerization, which in turn reduces the process inventory and the likelihood of catastrophic failures leading to instantaneous. However, the safety results also underscore that the catalytic column does not offer significant enhancements for instantaneous incidents, which can be explained by analyzing the operating conditions of the reactive column. It is crucial to note that the reactive distillation column demands higher pressure (15 atm) to facilitate some liquid-phase reactions, increasing the probability of pipeline ruptures and

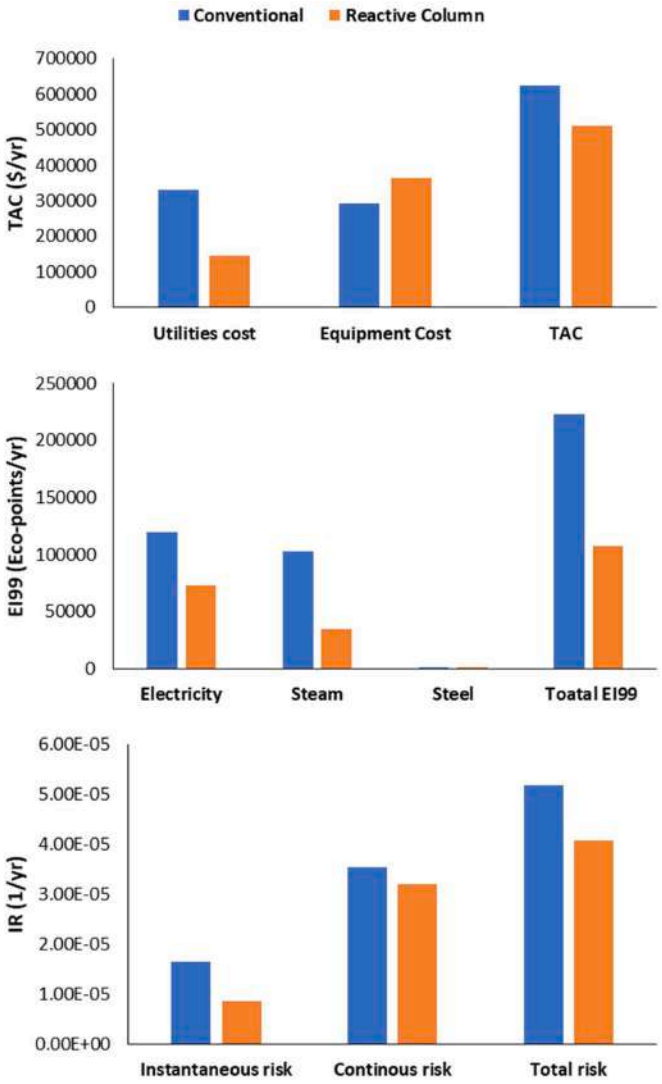

Fig. 6. Comparison of indicators results for conventional and intensifier oligomerization process.

subsequent flammable material leaks, raising the likelihood of accidents like jet fires, flash fires, and toxic releases.

6.2. *Proportional-integral control results*

Based on the previous results, the reactive distillation column offers interesting improvements compared to the conventional process. Some of the most important benefits include an increase in the production of heavier hydrocarbons like C12. Moreover, it offers significant and interesting improvements in other aspects such as costs, environmental impact, and safety. However, a final factor that must be evaluated to consider the catalytic column as a potential candidate to replace the conventional process is studying the control of the process. This evaluation aims to assess its ability to resist disturbances while maintaining safe operating conditions and ensuring product quality. In this section, the results are analyzed using feedback and model predictive control techniques for the reactive column.

As aforementioned, the parameter for the proportional integral controller (PI) were tuned using the minimization of IAE method. The results of the controller tuning are shown in Fig. S4 of the supplementary material. The control scheme is focused on controlling the composition of the most abundant compound in domes and bottoms of the reactive column, being in this case butene (C4) and dodecene (C12), respectively. The minimum IAE value for controlling C12 was found at 70 min for integral time and a gain of 10. The IAE became asymptotic and showed no significant improvement for gain values greater than or equal to 40. The optimal values for the butene controller were a gain of 30 and an integral time of 5 min. After tuning the controllers, they were simultaneously implemented in the catalytic distillation column. Different set-point changes and disturbances to manipulable variables were tested, with changes of 1 and 5 %, to analyze the control system's robustness and parameter tuning. The results of the disturbances for 1 and 5 % are shown in Figs. 7 and 8, respectively.

As shown in Figs. 7 and 8, the control system, using PI controllers, effectively manages disturbances and adjusts to 1 % setpoint changes, whether these are increases or. The system never requires more than 10 h to reach stability. However, it is important to note that despite reaching a stable state, the process dynamics are slow. Additionally, the system's reactions to all disturbances are noticeably oscillatory. This suggests that the controllers could be operating in an over-saturated state, indicating that the variables being controlled are working at their peak capacity.

When disturbances and 5 % set-point changes are introduced, the process does not always exhibit stable behavior. For instance, the control system was unable to manage a 5 % set-point change for butene, hence its graph is absent. Additionally, the control system failed to handle a 5 % disturbance in the feed flow. However, it is crucial to highlight that this control system can handle both negative and positive disturbances of 5 % for the reboiler duty. This capability is extremely significant from an operational and safety perspective. Given the exothermic nature of the reaction, changes in energy consumption, particularly increases in reboiler duty, could potentially lead to hazardous operations or accidents. It's also important to recognize that under this control system, the C12 composition in the bottoms is more sensitive to changes and displays a more oscillatory response. Despite this, the fluctuations in composition never exceed 5 %. On a positive note, the system successfully meets the required purity specifications for all the disturbance levels tested. This is crucial as maintaining these compositions is paramount to preserving the jet-fuel properties in downstream processes. Based on these results, it is concluded that the intensified process might be capable of operating under a conventional feedback control system.

6.3. *Model predictive control results*

Model predictive control consists of solving an optimization problem to predict and calculate optimal future process responses. The data for the state space model, which serves as the predictor model, were obtained from Aspen Dynamics. Random step changes were performed in the open loop on the manipulated variables, varying within +/- 10 % of their nominal value. These simulations spanned 295 h with a sampling time of 0.04 s, generating 7375 sampling points. Fig. 9(a) shows the step changes made to the reflux rate and the resulting dynamic responses of the output variables. This procedure was repeated for the other manipulated variables, including the condenser and reboiler duty and ethylene feed flow. The state space model was then constructed based on the dynamic responses to these step changes. The state space model obtained consists of 21 states, 3 outputs and 4 inputs. This model is presented in the supplementary material. Additionally, an accuracy test was performed to compare the dynamic responses of a nonlinear model (Aspen Dynamics simulation) and the linear model to random step changes. The accuracy test was performed for three output variables: top pressure, butene composition, and dodecane composition. The results of this accuracy test, focusing on disturbances in the reflux rate as a representative case, are shown in Fig. 9(b). It is important to note that both dynamic responses - linear and nonlinear - are very similar. In this case, the maximum difference between the two responses does not exceed 5 %. Based on the results, it is concluded that the state space model is suitable and can be used as a predictor. Accuracy tests results

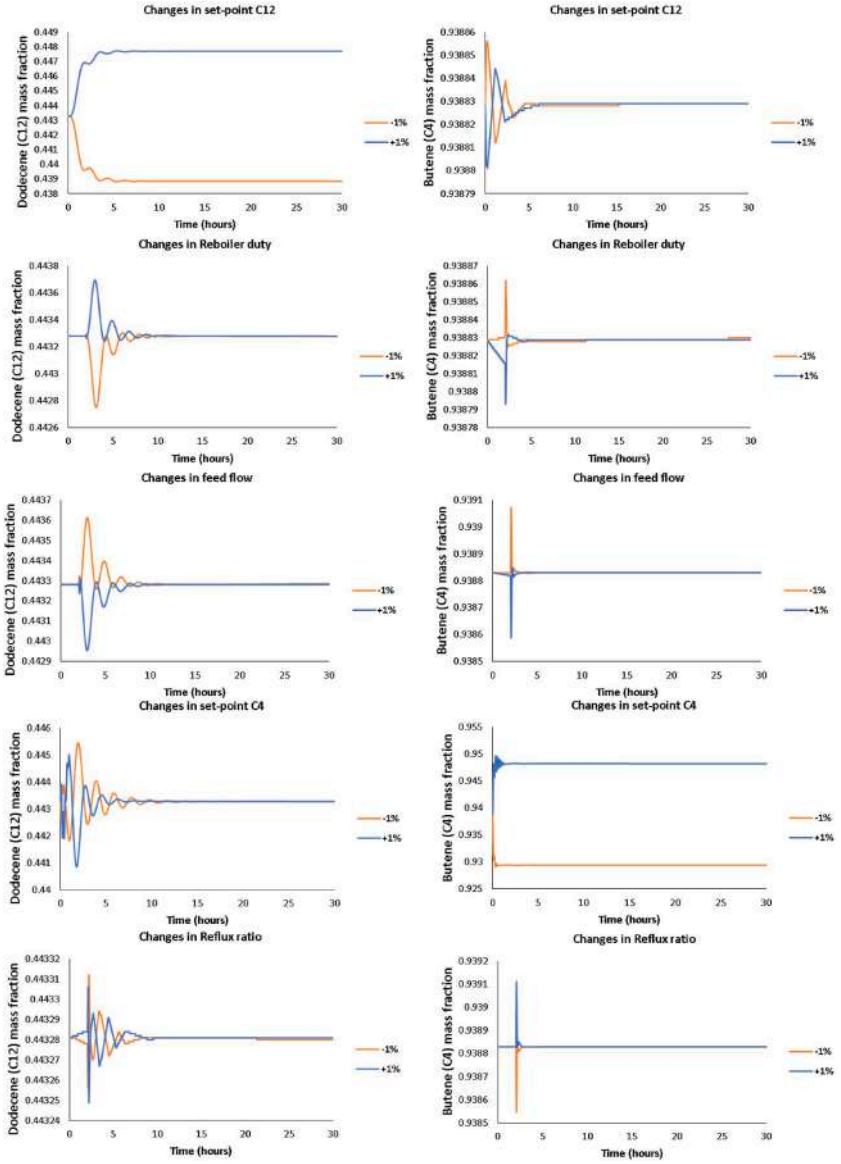

Fig. 7. Set -point changes and disturbances on manipulate variables using a PI controller.

by disturbing the reboiler duty, condenser duty, and ethylene feed rate are shown in the supplementary material (Figs. S5–S7).

The model predictive control (MPC) was implemented on a hybrid platform that links Aspen Dynamics with Simulink. Similar to PI controllers, the MPC controller also needs to be tuned. In this case, the tuning parameters are the weights of the objective function in Eq. (18). These parameters were tuned through a sensitivity analysis to minimize the sum of IAE for the dynamic responses of the butene and C12 loops, as there is no formal methodology for tuning the MPC parameters. Since the controller was designed using scaled variables ranging from 0 to 100, the weight tuning range was set from 10 to 0.01. This range was selected based on previous works [65]. The MPC controller parameters, obtained through the minimization of IAE method, are shown in Table 6.

Once the controller parameters were determined, similar to the PI controllers, disturbances of 5 % and 1 % were performed on the manipulated variables. The dynamic responses generated by this analysis are shown in Figs. 10 and 11. For small set point changes and disturbances, the MPC can control the process with fewer oscillations than the PI controllers. This might be because the MPC controllers do not oversaturate the control action as the controller is restricted to move the variables between 20 and 80 % of their capacity. Note that both the MPC and PI controllers generally stabilize the process in a similar time frame, often around 10 h. This suggests that the process has a very slow dynamic response but can be controlled without significant overshooting of compositions. As seen in Figs. 10 and 11, the MPC controller can control the process and stabilize the compositions around the nominal operating point for the compositions, but it may not precisely return exactly to the nominal value. However, the MPC maintains the compositions around the nominal operating point without significantly affecting the mixture's properties, especially at the bottoms. This was determined by calculating the TD86 boiling temperatures, which oscillated between 265 and 263 °C. Aspen Dynamics allows to calculate these temperature TD86.

The MPC controller is efficient at controlling the process for small disturbances of 1 %. However, its performance worsens for larger disturbances of 5 % (refer to Fig. 11), resulting in highly oscillatory responses and instability in many cases. This outcome was anticipated since the design of the MPC controller used a linear model, which typically offers better predictive accuracy for smaller disturbances. As the disturbance size increases, the linear predictor model's accuracy decreases, underscoring the need for nonlinear models in future work.

In order to objectively compare the controllers, Table 7 provides a

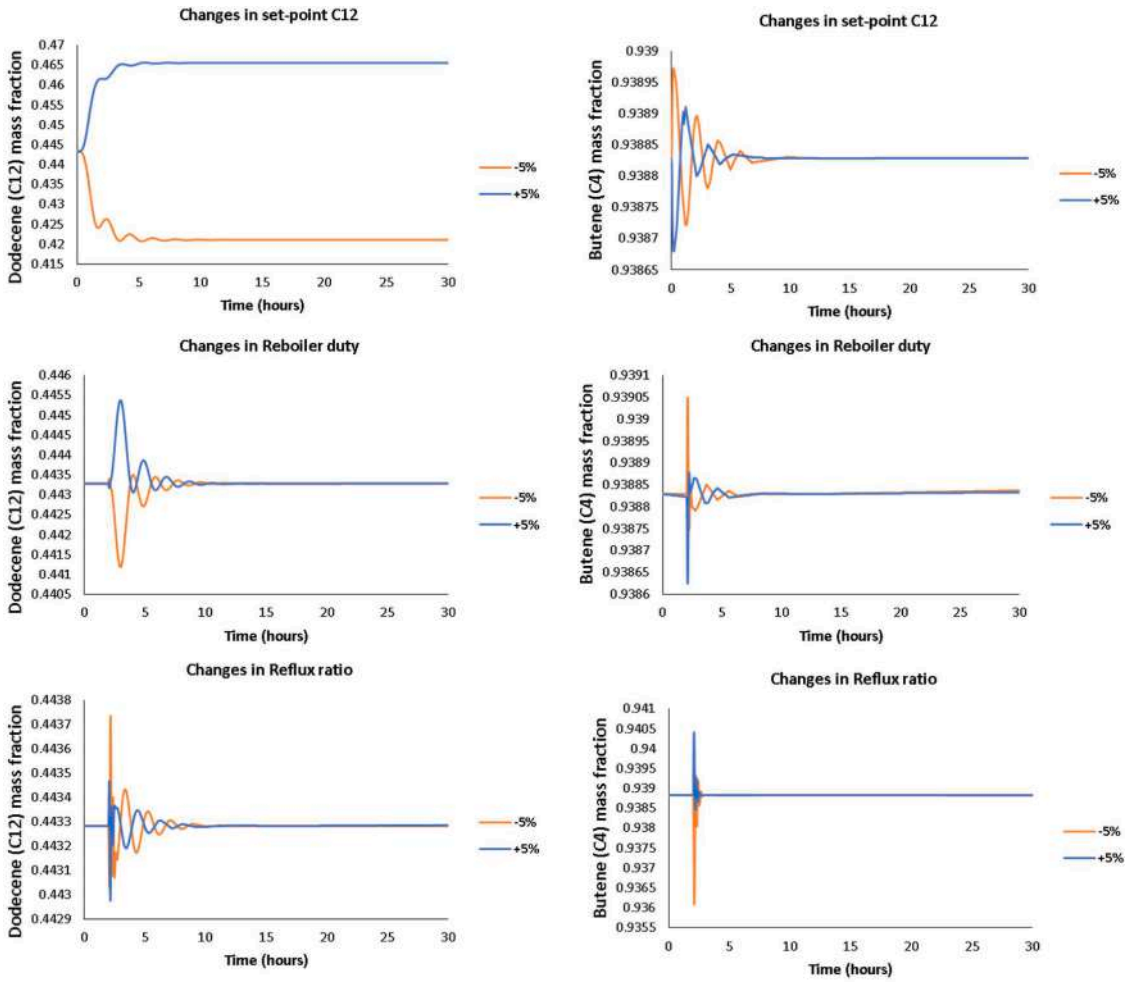

Fig. 8. Set-point changes and disturbances of 5 % using a PI controller.

comparison of the Integral Absolute Error (IAE) values for both loops. The table focuses solely on disturbances at 1 %, since the performance of the MPC controller decreases with higher disturbances. Additionally, Table 7 presents the average IAE from the 1 % disturbances, both positive and negative, simplifying the analysis of the results. Based on these results, a significant difference can be observed between the two types of controllers. For the butene composition control loop, the PI controller is superior, outperforming the MPC controller by up to 30 %. However, for the dodecene control loop, both controllers exhibit similar performance. For the bottom loop, the most significant difference arises when a disturbance in the ethylene feed flow is applied, while the performance for other disturbances remains similar. Thus, it has been concluded that the PI controller has the best performance for calculating the C4 composition, and for the bottom compositions, both controllers perform similarly.

Finally, based on the previous results for column control, choosing the most appropriate control strategy for the column is not a simple task, as it largely depends on personal preferences and specific control goals. Both control strategies - feedback control using PI controllers and predictive control - have their respective strengths and weaknesses. For a control scheme that is easy to implement and has a strong track record in the industry, the feedback control strategy using PI controllers might be the most effective choice. The process of tuning PI controllers is relatively straightforward, and there are many methods documented in existing literature. Moreover, these type of controllers and control strategies can overcome the deficiencies and effects of poor models [66]. However, one inherent drawback is a phenomenon known as reset windup. This occurs as a consequence of a large, sustained disturbance that is beyond the manipulated variable's range. In such cases, a physical limitation (like a control valve being fully open or completely closed) prevents the controller from reducing the error signal to zero. As a result, the feedback control becomes essentially disabled. On the other hand, this windup in predictive control can be easily avoided by adding constraints into the control problem. In this work, control actions are constrained between 20 % and 80 % of the variables' capacities. However, tuning a predictive controller is more complex due to the increased number of variables that require adjustment. These include prediction and control horizons, sampling time, and variable weights. The main disadvantage of the linear predictive control implemented in this work is that it performs well when dealing with minor disturbances below 1 %, as the process behavior in this range aligns more closely with linear behavior. However, for larger disturbances, its performance is affected because the linear predictor (state-space model) is not able to adequately predict the process behavior, resulting in more oscillatory responses from predictive control and degrading its performance [60]. Utilizing nonlinear models for the MPC predictor could potentially enhance the controller's performance, particularly in better controlling the compositions of the reactive column [66].

6.4. *Challenges of the reactive distillation column*

Up to now, the simulation results, both in steady-state and dynamic conditions (control simulations), have shown that it is technically feasible to replace the oligomerization stage in the ATJ process with reactive distillation, dramatically improving the selectivity of the hydrocarbons required for bio-jet fuel. However, there are some points that

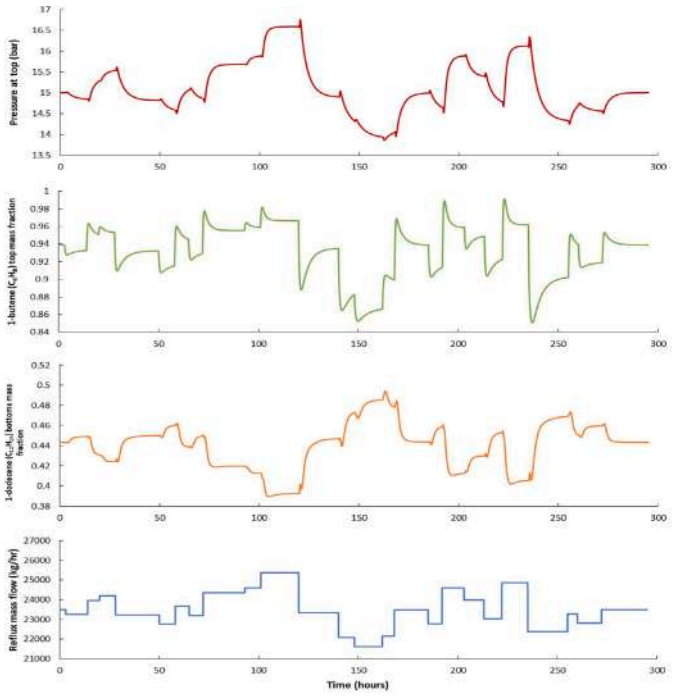

a)

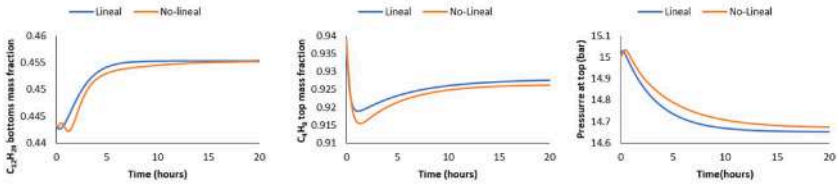

b)

Fig. 9. (a) Dynamic data used for system identification (b) Accuracy test results disturbing −1 % on reflux rate.

Table 6
Design parameter of oligomerization catalytic column.

Weights	Manipulate variables			Controlled variables		
	Condenser duty	Reboiler duty	Reflux rate	Top pressure	x_{C4}	x_{C12}
Output reference traking ($w_{i,j}^{y}$)	–	–	–	1	1	2
Manipulate variable tracking ($w_{i,j}^{u}$)	0	0	0	–	–	–
Move suppression ($w_{i,j}^{\Delta u}$)	0.5	1	1.3	–	–	–
Prediction horizon		Control horizon		Sample Time		
50 intervals		10 intervals		3 min		

need to be discussed and cannot be deeply addressed with Aspen Plus simulations.

While the catalyst does not require prior activation but only reaching the required oligomerization temperature [32,34], we consider that the main challenge of this column lies in obtaining an appropriate catalyst support or distribution that allows achieving the required holdup in the reactive distillation column. Holdup is a crucial parameter in the reactive distillation process as it is associated with the residence time of the reactants for the reaction to occur. In this regard, considering the dimensions of the column, we believe that the required holdups to obtain the desired hydrocarbons are relatively small (indicating a short residence time), which poses a challenge in designing the catalyst to achieve these holdups. These holdups depend largely on the diameter of the column and the liquid height. A small holdup implies a small liquid height, which can lead to operational issues such as stage dry-out [22]. In this regard, the use of Computational Fluid Dynamics (CFD) techniques will be indispensable to find a suitable way to properly pack the reactive stages.

Additionally, in the oligomerization process, pressure plays an important role, so the catalyst shape should also be a factor to consider for successful implementation. Therefore, we believe that the principal challenge for the implementation of this process relies heavily on the adequate catalyst design.

7. Conclusions

In this work, a novel reactive distillation column was proposed to improve the oligomerization stage of the ATJ process. To evaluate the

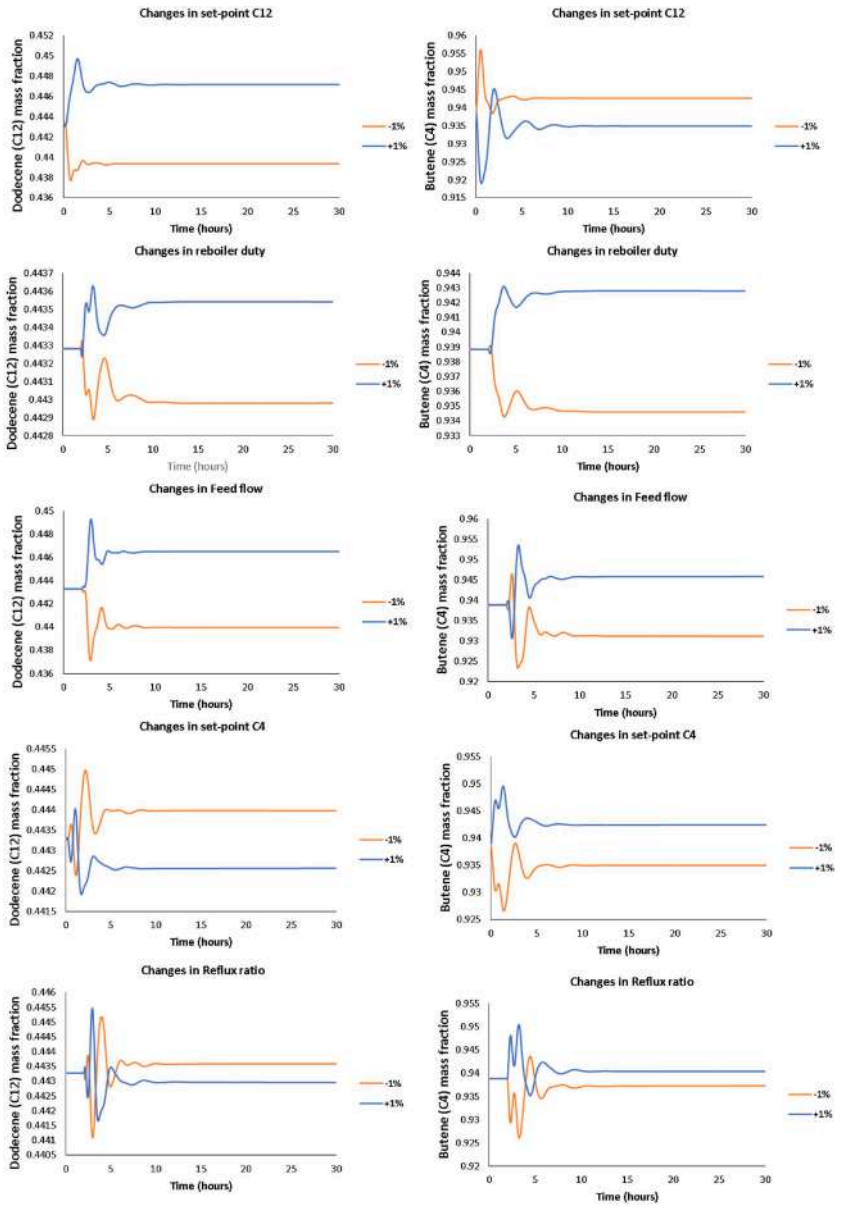

Fig. 10. Set-point changes and disturbances of 1 % using MPC.

benefits of this equipment, it was compared to its conventional counterpart in economic, environmental, and safety terms. The results indicate that the intensified process offers savings in TAC of around 19 % compared to the conventional one, primarily due to significant reductions in utility costs. This includes less usage of cooling services, lower electricity consumption for pumping and compression, and overall energy savings. In terms of environmental impact, the intensified process has a smaller eco-indicator, resulting from reduced energy usage. Specifically, it leads to 40 % and 60 % fewer eco-points when using electricity and steam, respectively. From a safety perspective, the intensified process is safer, with a reduced accident risk of up to 22 %. This is mainly due to the use of fewer pieces of equipment, which reduces process inventory and the likelihood of catastrophic failures. A control study was conducted using proportional integral controllers and model predictive control to assess the feasibility of operating this column. The results demonstrated that it is possible to control this intensified equipment using both control strategies. However, the performance of MPC control was not superior when compared to the traditional proportional integral controller. This can be attributed to the fact that the linear model used for MPC control was not robust enough to capture the non-linearity of the reactive column. Therefore, it is concluded that, for this case, conventional control using PI controllers is better, as it exhibits performance up to 30 % higher than MPC when considering IAE as a metric. For future work, it is recommended to use combined design and optimization techniques to improve the design of the intensified column. It is also suggested to incorporate non-linear model predictive control to enhance the performance of the predictive controller, particularly for disturbances greater than 1 %. In this context, exploring the use of non-linear models with artificial neural networks could be a valuable alternative due to their high accuracy and rapid problem-solving.

CRediT authorship contribution statement

Gabriel Contreras-Zarazúa: Conceptualization, Methodology, Software, Writing – original draft, Investigation. **Eduardo Sánchez-Ramirez:** Conceptualization, Writing – review & editing. **Esteban Abelardo Hernández-Vargas:** Conceptualization, Validation, Investigation, Writing – review & editing. **Juan Gabriel Segovia-Hernández:** Resources, Writing – review & editing. **Juan José Quiroz Ramírez:**

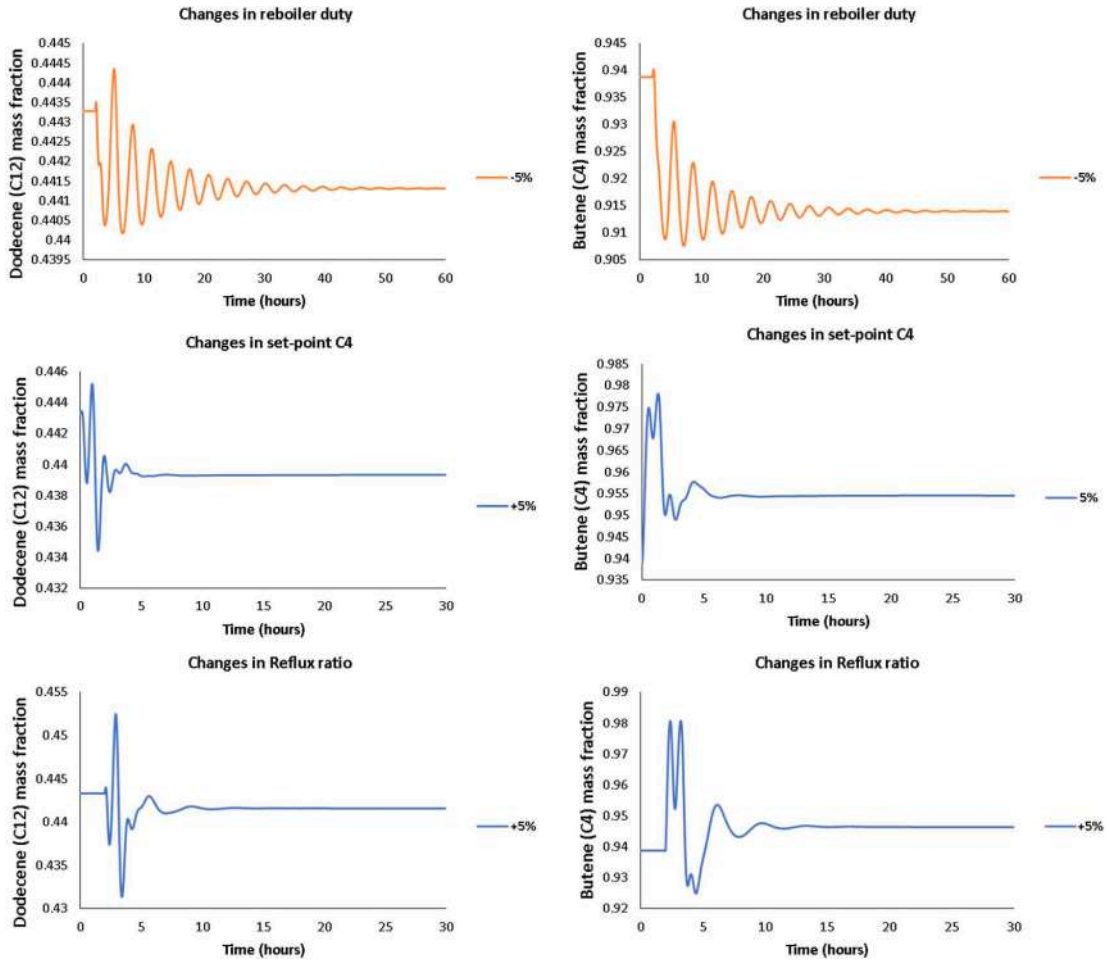

Fig. 11. Set-point changes and disturbances of 5 % using MPC.

Table 7
Average IAE values for disturbances of 1 %.

Control loop	Reboiler duty disturbance	Reflux rate disturbance	Feed flow disturbance	C12 set-point change	C4 set-point change
C4 control loop (PI)	2.86e-5	32.70e-5	3.4632e-5	3.88e-5	9.501e-5
C4 control loop (MPC)	0.1091	0.05802	0.3016	0.1268	0.1648
C12 control loop (PI)	0.0010875	3.8409e-5	4.5924e-4	0.006075	0.004456
C12 control loop (MPC)	0.00794	0.01086	0.1357	0.06675	0.1323
Difference C4 loop	10.90 %	5.7693 %	30.15 %	12.67 %	16.47 %
Difference C12 loop	0.68 %	1.082 %	13.52 %	6.06 %	12.78 %

Conceptualization, Validation, Investigation, Writing – review & editing.

Declaration of Competing Interest

The authors declare that they have no known competing financial interests or personal relationships that could have appeared to influence the work reported in this paper.

Data availability

The authors are unable or have chosen not to specify which data has been used.

Supplementary materials

Supplementary material associated with this article can be found, in the online version, at doi:10.1016/j.cep.2023.109548.

References

[1] U.S. Energy Information Administration, U.S. energy facts explained, (2022). https://www.eia.gov/energyexplained/us-energy-facts/.
[2] C. Gutiérrez-Antonio, M.L. Soria Ornelas, F.I. Gómez-Castro, S. Hernández, Intensification of the hydrotreating process to produce renewable aviation fuel through reactive distillation, Chem. Eng. Process. Process Intensif. 124 (2018) 122–130, https://doi.org/10.1016/j.cep.2017.12.009.
[3] U.S. Department of Energy, The role of fossil energy and carbon management in achiving net-zero greenhouse gas emissions, 2022. https://www.nrel.gov/docs/fy21osti/79444-8.pdf.
[4] National Renewable Energy Laboratory (NREL), Chapter 8. Greenhouse gas emissions., 2021.
[5] International Air Transport Association (IATA), Air passenger numbers to recover in 2024, (2022). https://www.iata.org/en/pressroom/2022-releases/2022-03-01-01/(accessed August 1, 2022).
[6] I.R.E.A. (IRENA), Reaching zero with renewables biojet fuels, 2021. https://www.irena.org/-/media/Files/IRENA/Agency/Publication/2021/Jul/IRENA_Reaching_Zero_Biojet_Fuels_2021.pdf.

[7] E. Martinez-Hernandez, L.F. Ramírez-Verduzco, M.A. Amezcua-Allieri, J. Aburto, Process simulation and techno-economic analysis of bio-jet fuel and green diesel production — Minimum selling prices, Chem. Eng. Res. Des. 146 (2019) 60–70, https://doi.org/10.1016/j.cherd.2019.03.042.

[8] A.G. Romero-Izquierdo, F.I. Gómez-Castro, C. Gutiérrez-Antonio, S. Hernández, M. Errico, Intensification of the alcohol-to-jet process to produce renewable aviation fuel, Chem. Eng. Process. Process Intensif. 160 (2021) 1–11, https://doi.org/10.1016/j.cep.2020.108270.

[9] Q. Tan, Y. Cao, J. Li, Prepared multifunctional catalyst Ni2P/Zr-SBA-15 and catalyzed Jatropha Oil to produce bio-aviation fuel, Renew. Energy 150 (2020) 370–381, https://doi.org/10.1016/j.renene.2019.12.029.

[10] J. Liao, Q. Zhong, J. Gu, S. Qiu, Q. Meng, Q. Zhang, T. Wang, New approach for bio-jet fuels production by hydrodeoxygenation of higher alcohols derived from C-C coupling of bio-ethanol, Appl. Energy 324 (2022), 119843, https://doi.org/10.1016/j.apenergy.2022.119843.

[11] V.L. Dagle, J.S. Lopez, A. Cooper, J. Luecke, M. Swita, R.A. Dagle, D. Gaspar, Production and fuel properties of iso-olefins with controlled molecular structure and obtained from butene oligomerization, Fuel 277 (2020), 118147, https://doi.org/10.1016/j.fuel.2020.118147.

[12] J. Saavedra Lopez, R.A. Dagle, V.L. Dagle, C. Smith, K.O. Albrecht, Oligomerization of ethanol-derived propene and isobutene mixtures to transportation fuels: catalyst and process considerations, Catal. Sci. Technol. 9 (2019) 1117–1131, https://doi.org/10.1039/c8cy02297f.

[13] K.P. Brooks, L.J. Snowden-Swan, S.B. Jones, M.G. Butcher, G.-S.J. Lee, D. M. Anderson, J.G. Frye, J.E. Holladay, J. Owen, L. Harmon, F. Burton, I. Palou-Rivera, J. Plaza, R. Handler, D. Shonnard, Low-Carbon Aviation Fuel Through the Alcohol to Jet Pathway, Elsevier Inc., 2016, https://doi.org/10.1016/b978-0-12-804568-8.00006-8.

[14] J.A. Vazquez-Castillo, G. Contreras-Zarazua, J.G. Segovia-Hernandez, Heat-integrated reactive distillation processes to produce ethyl levulinate: design and optimization including environmental, Saf. Econ. Asp. (2019), https://doi.org/10.1016/B978-0-12-818634-3.50060-6.

[15] R. Taylor, R. Krishna, Modelling reactive distillation, Chem. Eng. Sci. 55 (2000) 5183–5229, https://doi.org/10.1016/S0009-2509(00)00120-2.

[16] K. Sundmacher, A. Kienle. Reactive Distillation Status and Future Directions, Wiley, 2002.

[17] J.A. Moulijn, A. Stankiewicz, Process Intensification, in: V. Strezov, J. Zoeller, M. Abraham (Eds.), Encyclopedia of Sustainable Technologies - Volume 3 Vol. 3, 2017, pp. 509–518, https://doi.org/10.1016/B978-0-12-409548-9.10242-8.

[18] G. Contreras-Zarazúa, J.A. Vázquez-Castillo, C. Ramírez-Márquez, J.G. Segovia-Hernández, J.R. Alcántara-Ávila, Multi-objective optimization involving cost and control properties in reactive distillation processes to produce diphenyl carbonate, Comput. Chem. Eng. 105 (2017), https://doi.org/10.1016/j.compchemeng.2016.11.022.

[19] G. Contreras-Zarazúa, J.A. Vázquez-Castillo, C. Ramírez-Márquez, G.A. Pontis, J. G. Segovia-Hernández, J.R. Alcántara-Ávila, Comparison of intensified reactive distillation configurations for the synthesis of diphenyl carbonate, Energy 135 (2017), https://doi.org/10.1016/j.energy.2017.06.156.

[20] C. Ramírez-Márquez, G. Contreras-Zarazúa, J.A. Vázquez-Castillo, F. López-Caamal, H. Hernández-Escoto, J.R. Alcántara-Ávila, J.G. Segovia-Hernández, Operability and proportional integral control of reactive distillation configurations, Ind. Eng. Chem. Res. 58 (2019) 18267–18279, https://doi.org/10.1021/acs.iecr.9b02678.

[21] N. Sharma, K. Singh, Control of reactive distillation column: a review, Int. J. Chem. React. Eng. 8 (2010), https://doi.org/10.2202/1542-6580.2260.

[22] W.L. Luyben, C.C. Yu. *Reactive distillation design and control*, John Wiley & Sons, 2009.

[23] ASTM International. ASTM D7566—21, Standard Specifica-tion for Aviation Turbine Fuel Containing Synthesized Hydro-carbons, ASTM International (2021), https://doi.org/10.1520/D7566-21.operated.

[24] S. Geleynse, K. Brandt, M. Garcia-Perez, M. Wolcott, X. Zhang, The alcohol-to-jet conversion pathway for drop-in biofuels: techno-economic evaluation, ChemSusChem 11 (2018) 3728–3741, https://doi.org/10.1002/cssc.201801690.

[25] W.C. Wang, L. Tao, Bio-jet fuel conversion technologies, Renew. Sustain. Energy Rev. 53 (2016) 801–822, https://doi.org/10.1016/j.rser.2015.09.016.

[26] N. Zhan, Y. Hu, H. Li, D. Yu, Y. Han, H. Huang, Lanthanum-phosphorous modified HZSM-5 catalysts in dehydration of ethanol to ethylene: a comparative analysis, Catal. Commun. 11 (2010) 633–637, https://doi.org/10.1016/j.catcom.2010.01.011.

[27] A. Jonathan, E.G. Tomashek, M.P. Lanci, J.A. Dumesic, G.W. Huber, Reaction kinetics study of ethylene oligomerization into linear olefins over carbon-supported cobalt catalysts, J. Catal. 404 (2021) 954–963, https://doi.org/10.1016/j.jcat.2021.05.035.

[28] A.M. Al-Jarallah, J.A. Anabtawi, M.A.B. Siddiqui, A.M. Aitani, A.W. Al-Sa'doun, Ethylene dimerization and oligomerization to butene-1 and linear α-olefins: a review of catalytic systems and processes, Catal. Today 14 (1992) 1–124.

[29] A. Jonathan, N.M. Eagan, D.L. Bruns, S.S. Stahl, M.P. Lanci, J.A. Dumesic, G. W. Huber, Ethylene oligomerization into linear olefins over cobalt oxide on carbon catalyst, Catal. Sci. Technol. 11 (2021) 3599–3608, https://doi.org/10.1039/d1cy00207d.

[30] E.C. Carlson, Don't gamble with physical properties for simulations, Chem. Eng. Prog. (1996) 35–46. http://www.cchem.berkeley.edu/cbe150b/docs/VLE/Guidelines.pdf.

[31] R.M. Rivas-Interian, E. Sanchez-Ramirez, J.J. Quiroz-Ramírez, J.G. Segovia-Hernandez, Feedstock planning and optimization of a sustainable distributed configuration biorefinery for biojet fuel production via ATJ process, Biofuel Bioprod Biorefin 17 (1) (2023) 71–96.

[32] M.D. Heydenrych, C.P. Nicolaides, M.S. Scurrell, Oligomerization of ethene in a slurry reactor using a nickel(II)-exchanged silica-alumina catalyst, J. Catal. 197 (2001) 49–57, https://doi.org/10.1006/jcat.2000.3035.

[33] E. Sánchez-Ramírez, B. Huerta-Rosas, J.J. Quiroz-Ramírez, V.A. Suárez-Toriello, G. Contreras-Zarazua, J.G. Segovia-Hernández, Optimization-based framework for modeling and kinetic parameter estimation, Chem. Eng. Res. Des. 186 (2022) 647–660, https://doi.org/10.1016/j.cherd.2022.08.040.

[34] J. Heveling, A. van der Beek, M. de Pender, Oligomerization of ethene over nickel-exchanged zeolite y into a diesel-range product, Appl. Catal. 42 (1988) 325–336, https://doi.org/10.1016/0166-9834(88)80011-3.

[35] H.S. Fogler. Elements of Chemical Reaction Engineering, Pearson, 2019.

[36] J. Yang, Z. Xin, Q. (Sophia) He, K. Corscadden, H. Niu, An overview on performance characteristics of bio-jet fuels, Fuel 237 (2019) 916–936, https://doi.org/10.1016/j.fuel.2018.10.079.

[37] J. Li, G. Yang, Y. Yoneyama, T. Vitidsant, N. Tsubaki, Jet fuel synthesis *via* Fischer–Tropsch synthesis with varied 1-olefins as additives using Co/ZrO_2-SiO_2 bimodal catalyst, Fuel 171 (2016) 159–166, https://doi.org/10.1016/j.fuel.2015.12.062.

[38] M.A. Al-Arfaj, W.L. Luyben, Design and control of an olefin metathesis reactive distillation column, Chem. Eng. Sci. 57 (2002) 715–733, https://doi.org/10.1016/S0009-2509(01)00442-0.

[39] K. Cheng, S.J. Wang, D.S.H. Wong, Steady-state design of thermally coupled reactive distillation process for the synthesis of diphenyl carbonate, Comput. Chem. Eng. 52 (2013) 262–271, https://doi.org/10.1016/j.compchemeng.2013.02.001.

[40] C. Jiménez-González, D.J. Constable, Green Chemistry and Engineering: A Practical Design Approach, John Wiley & Sons, 2011, pp. 1–680.

[41] R. Turton, R.C. Bailie, W.B. Whiting, J.A. Shaeiwitz, Analysis, Synthesis and Design of Chemical Processes, Pearson Education, 2018, pp. 1–1200.

[42] M. Goedkoop, R. Spriensma, The Eco-indicator 99, a damage oriented method for Life Cycle Impact Assessment, methodology report, PRe Consultants BV (2001), 132 pp.

[43] G. Contreras-Zarazúa, M. Martin-Martin, E. Sánchez-Ramirez, J.G. Segovia-Hernández, Furfural production from agricultural residues using different intensified separation and pretreatment alternatives. Economic and environmental assessment, Chem. Eng. Process. Process Intensif. 171 (2022), https://doi.org/10.1016/j.cep.2021.108569.

[44] E. Sánchez-Ramírez, J.J. Quiroz-Ramírez, J.G. Segovia-Hernández, S. Hernández, J.M. Ponce-Ortega, Economic and environmental optimization of the biobutanol purification process, Clean Technol. Environ. Policy 18 (2016) 395–411, https://doi.org/10.1007/s10098-015-1024-8.

[45] M. Errico, E. Sanchez-Ramirez, J.J. Quiroz-Ramìrez, J.G. Segovia-Hernandez, B. G. Rong, Synthesis and design of new hybrid configurations for biobutanol purification, Comput. Chem. Eng. 84 (2016) 482–492, https://doi.org/10.1016/j.compchemeng.2015.10.009.

[46] J.J. Quiroz-Ramírez, E. Sánchez-Ramírez, S. Hernández-Castro, J.G. Segovia-Hernández, J.M. Ponce-Ortega, Optimal planning of feedstock for butanol production considering economic and environmental aspects, ACS Sustain. Chem. Eng. 5 (2017) 4018–4030, https://doi.org/10.1021/acssuschemeng.7b00015.

[47] Pré Consultants. The Eco-indicator 99 – A damage oriented method for Life Cycle Impact Assessment, Methodology Annex, Ministry of Housing, Spatial Planning and the Environment, The Hague, Netherlands, 2001.

[48] Center for. Chemical Process Safety (CCPS), Guidelines for Chemical Process Quantitative Risk Analysis, Center for Chemical Process Safety of the, American Institute of Chemical Engineers, AICHE,2000.

[49] D.A. Crowl, J.F. Louvar. Chemical and Process Safety Fundamentals with Applications, Prentice Hall, 2012, https://doi.org/10.1021/op3003322.

[50] W.L. Luyben, Distillation Design and Control using Aspen Simulation, 2nd Edi, Wiley-AIChE, 2013.

[51] S. Skogestad, K. Havre, The use of RGA and condition number as robustness measures, Comput. Chem. Eng. 20 (1996) 1005–1010, https://doi.org/10.1016/0098-1354(96)00175-5.

[52] M.M. Skogestad Sigurd, LV- control of a high purity distillation column, Chem. Eng. Sci. 72 (1988) 1055–1065, https://doi.org/10.1002/cjce.5450720617.

[53] C. Ramírez-Márquez, G. Contreras-Zarazúa, J.A. Vázquez-Castillo, F. López-Caamal, H. Hernández-Escoto, J.R. Alcántara-Ávila, J.G. Segovia-Hernández, Operability and proportional integral control of reactive distillation configurations, Ind. Eng. Chem. Res. 58 (2019), https://doi.org/10.1021/acs.iecr.9b02678.

[54] M. Schwenzer, M. Ay, T. Bergs, D. Abel, Review on model predictive control: an engineering perspective, Int. J. Adv. Manuf. Technol. 117 (2021) 1327–1349, https://doi.org/10.1007/s00170-021-07682-3.

[55] M. Morari, C.E. Garcia, D.M. Prett, Model predictive control: theory and practice, IFAC Proc. 21 (1988) 1–12, https://doi.org/10.1016/b978-0-08-035735-5.50006-1. Vol.

[56] R.R. Interan, Optimización De Sistemas Intensificados Para La Producción De Bioturbosina A Través De Alcoholes De Forma Sustentable, Universidad de Guanajuato, 2021.

[57] T.A.B. Joe Qin, An overview of nonlinear model predictive control, Prog. Syst. Control Theory 402 (2000) 107–117, https://doi.org/10.1007/978-1-84996-071-7_7.

[58] Q. Li, W. Zhang, Y. Qin, A. An, Model predictive control for the process of mea absorption of CO_2 based on the data identification model, Processes 9 (2021) 1–16, https://doi.org/10.3390/pr9010183.

[59] T. Sultan, H. Zabiri, M. Shahbaz, A.S. Maulud, Performance evaluation of the fast model predictive control scheme on a CO_2 capture plant through absorption/stripping system, Process Saf. Environ. Prot. 157 (2022) 218–236, https://doi.org/10.1016/j.psep.2021.11.018.
[60] J. Eggins, Integration of MATLAB and LabVIEW with aspen plus dynamics using control strategies for a high-fidelity distillation column, Murdoch University, 2015. https://researchrepository.murdoch.edu.au/id/eprint/29841/1/whole.pdf.
[61] O.L. Sydora, Selective ethylene oligomerization, Organometallics 38 (2019) 997–1010, https://doi.org/10.1021/acs.organomet.8b00799.
[62] G.J.P. Britovsek, R. Malinowski, D.S. McGuinness, J.D. Nobbs, A.K. Tomov, A. W. Wadsley, C.T. Young, Ethylene oligomerization beyond Schulz–Flory distributions, ACS Catal. 5 (2015) 6922–6925, https://doi.org/10.1021/acscatal.5b02203.
[63] H. Wei, W. Liu, X. Chen, Q. Yang, J. Li, H. Chen, Renewable bio-jet fuel production for aviation: A review, Fuel 254 (2019) 115599, https://doi.org/10.1016/j.fuel.2019.06.007.
[64] G. Thomassen, M. Van Dael, S. Van Passel, F. You, How to assess the potential of emerging green technologies? Towards a prospective environmental and techno-economic assessment framework, Green Chem. 21 (2019) 4868–4886, https://doi.org/10.1039/c9gc02223f.
[65] MATLAB, Design and cosimulate control of high-fidelity distillation tower with aspen plus dynamics, (2022). https://la.mathworks.com/help/mpc/ug/design-and-cosimulate-control-of-high-fidelity-distillation-tower-with-aspen-plus-dynamics.html.
[66] D.E. Seborg, T.F. Edgar, D.A. Mellichamp, F.J. Doyle III, Process Dynamics and Control, Wiley, 2019 fourth edition.